agronomy

MDPI

Review

Understanding Starch Structure: Recent Progress

Eric Bertoft

Bertoft Solutions, Gamla Sampasvägen 18, 20960 Turku, Finland; eric.bertoft@abo.fi

Academic Editor: Ian J. Tetlow
Received: 25 July 2017; Accepted: 22 August 2017; Published: 25 August 2017

Abstract: Starch is a major food supply for humanity. It is produced in seeds, rhizomes, roots and tubers in the form of semi-crystalline granules with unique properties for each plant. Though the size and morphology of the granules is specific for each plant species, their internal structures have remarkably similar architecture, consisting of growth rings, blocklets, and crystalline and amorphous lamellae. The basic components of starch granules are two polyglucans, namely amylose and amylopectin. The molecular structure of amylose is comparatively simple as it consists of glucose residues connected through α-(1,4)-linkages to long chains with a few α-(1,6)-branches. Amylopectin, which is the major component, has the same basic structure, but it has considerably shorter chains and a lot of α-(1,6)-branches. This results in a very complex, three-dimensional structure, the nature of which remains uncertain. Several models of the amylopectin structure have been suggested through the years, and in this review two models are described, namely the "cluster model" and the "building block backbone model". The structure of the starch granules is discussed in light of both models.

Keywords: starch granules; amylose; amylopectin; cluster model; building block backbone model

1. Introduction

Starch constitutes a major energy supply for humans worldwide and is produced as a reserve carbohydrate in plants. The most important sources for humans are diverse cereals, rhizomes, roots and tubers. Storage starch is produced in amyloplasts as discrete granules with distinct morphology in different plants, ranging from round, oval, ogival or elongated to flat, lenticular or polyhedral, and sizes from sub-microns to more than 100 μm in diameter [1]. In some cereals, notably wheat and barley, there are two major populations of granules distinguished by their size; the diameter cut-off being approximately at 10 μm [2–4]. In barley, the average diameter of the large granules (also called A-granules) is between 15 and 19 μm depending on the variety, and the diameter of the small (B) granules is between 3.1–3.7 μm [5].

The starch granules consist almost entirely of two major polysaccharides, namely amylose and amylopectin. Both consist of chains of α-(1,4)-linked D-glucose residues, which are interconnected through α-(1,6)-glucosidic linkages, thus forming branches in the polymers. Although amylose traditionally is considered to be linear, branched amylose molecules contains few branches [6], but both branched and linear amylose have long chains with several hundreds or even thousand glucosyl units [7,8], whereas amylopectin is extensively branched and have comparatively short chains [9,10]. The branches in amylopectin constitute about 5% of the molecule, which results in a very complex molecular structure. Short chains of amylopectin form double-helices, which crystalize and contribute to the semi-crystalline nature of the starch granules [11]. In most "normal" starch granules, amylopectin constitutes the major component by weight, whereas amylose constitutes 15–30%; however, many exceptions exist. Waxy starches, so named because of the waxy appearance of the endosperm in waxy cereals, contain no or very little amylose. Genetically modified starches may contain 50–80% amylose [12–15]. A report presented recently an engineered barley starch reaching almost 100% apparent amylose [16].

In addition to amylose and amylopectin, some starches, notably from mutant plants, contain so-called intermediate materials in various amounts [17–20]. As the name indicates, these polyglucans have structures that are in between that of amylose and amylopectin [18,21–23]. Intermediate materials have attained interest because they appear to be the result of an altered biosynthesis in the mutant plants. Indeed, intermediate material was found in wheat starch granules during endosperm development [24]. The study of the structure of intermediate materials might therefore be helpful in understanding starch biosynthesis and the contribution of the enzymes involved in the process.

Minor non-carbohydrate compounds in starch granules contribute at most only a few per cent by weight. Proteins in the granules are mostly related to the biosynthesis of the starch. Some proteins are only loosely associated with the granules, whereas others are firmly bound inside the granules, notably granule-bound starch synthase I (GBSSI), which is required for amylose synthesis [25–29]. Lipids are rare in many root and tuber starches [30,31], but more abundant in cereals in the form of free fatty acids or lysophospholipids, which make inclusion complexes with amylose [32–35]. In many root and tuber starches, especially potato, the phosphate is not associated with lipids, however, but covalently bound to the amylopectin component [36–39]. In contrast, cereal and grass starches have only very little covalently bound phosphate. Nevertheless, this phosphate is important as it is involved in starch turnover in the plant [40]. In addition to phosphorus, trace amounts of other elements are also found, of which potassium and magnesium are comparatively abundant [41].

This review highlights the present knowledge of the structure of the starch granule and its two major components, amylose and amylopectin. A special focus is devoted to a new model of amylopectin structure and its impact on our understanding of starch properties and biosynthesis.

2. The Starch Granule

In view of the great diversity in starch granule morphology, it is remarkable to find that their internal architectural features are shared universally among the plants and regardless the plant organ (endosperm, root, stem, etc.). When observed in cross-polarized light in an optical microscope, a "Maltese cross" is typically seen extending the arms from the so-called hilum, which is believed to be the origin of growth of the granule [42–44]. This birefringence pattern shows that the molecules, or a large part of the molecules, are arranged in a radial fashion and suggests a high degree of order inside the granules (Figure 1) [45].

2.1. Crystallinity

As mentioned above, starch granules are semi-crystalline, i.e., they contain both crystalline and amorphous parts. If starch granules are treated in dilute hydrochloric acid, or sulphuric acid, the amorphous parts in the granules are removed and the crystalline parts remain [46,47]. The "Maltese cross" also remains [48], which shows that the organized molecular segments are confined to the crystallites. The crystallites are formed by short, external chain segments of amylopectin with a degree of polymerization (DP) approximately 10–20 glucosyl units [49–52]. As two chains unite into a double-helix with 6 glucose residues per turn of each strand and a pitch of 2.1 nm [53], the length of these double-helices is about 4~6 nm. Wide-angle X-ray scattering (WAXS, also known as X-ray diffraction, XRD) has shown that the double-helices crystallises into either of two polymorphs, the so-called A- or B-types (Figure 1). Some plants, such as peas and many other legumes, possess granules with a mixed pattern assigned C-type [42,54–56]. In the A-type crystal, the double-helices are closely packed into a monoclinic unit cell (with dimensions a = 20.83 Å, b = 11.45 Å, c = 10.58 Å, space group B2) containing 8 water molecules [57]. In the B-type crystal, the double-helices are packed in a hexagonal unit cell (dimensions $a = b$ = 18.5 Å, c = 10.4 Å, space group $P6_1$) with 36 water molecules [58]. In this crystalline lattice the water molecules fill up a channel, which does not exist in the A-type. The relative crystallinity in starch granules greatly varies between plant varieties in the range 17~50%, most often being higher in waxy starches compared to their normal, amylose-containing counterparts [9,59–63].

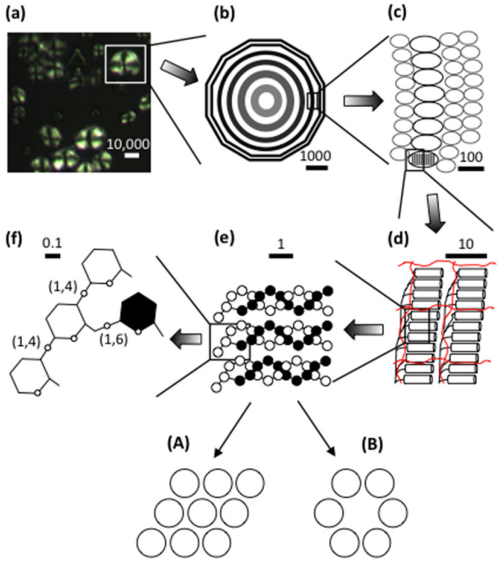

Figure 1. Dimensions in starch: from granules to glucosyl units. (**a**) Maize starch granules observed under polarised light showing the "Maltese cross", which is indicative of a radial organisation within the starch granule. (**b**) A hypothetical granule (in this case polyhedral) with growth rings extending from the hilum. (**c**) Blocklets in semi-crystalline (black) and amorphous (grey) rings. (**d**) Crystalline and amorphous lamellae formed by double helices (cylinders) and branched segments of amylopectin (black lines), respectively. Amylose molecules (red lines) are interspersed among the amylopectin molecules. (**e**) Three double-helices of amylopectin. Each double-helix consists of two polyglucosyl chains, in which the glucosyl residues are symbolised by white and black circles, respectively. The double helices form either A- or B-polymorphic crystals (A and B, respectively, in which the circles symbolises the double helices seen from the edge). (**f**) Glucosyl units showing α-(1,4)- and α-(1,6)-linkages at the base of the double-helix. The bar scale (in nm) is only approximate to give an impression of the size dimensions.

2.2. Lamellar Structure

Small-angle X-ray scattering (SAXS) shows a 9–10 nm repeat distance in all starch granules [54,64,65]. This was suggested to stem from stacks of repeating crystalline and amorphous lamellae, of which the former are represented by the double-helices (Figure 1) [66]. The crystalline lamellae have been isolated from acid-treated granules. In transmission electron microscopy (TEM) images, waxy maize granules with A-type crystallinity show regularly formed parallelepipedal blocks having acute angles of 60~65° and with lengths and widths of 20–40 and 15–30 nm, respectively [67]. The dimensions suggest that a single nanocrystal contains between 150 and 300 double-helices [68]. Amylose-containing starches give rise to nanocrystals with less perfect symmetry, suggesting interference of amylose on the crystal structure. Nanocrystals isolated from B-type starch granules (e.g., potato granules) possess irregular structures, probably a result of the organisation of the double-helices in the B-crystallites [48]. As the repeat distance is 9–10 nm and the crystalline lamellae fill up 4–6 nm, the amorphous lamellae are 3–6 nm thick. This part consists of longer, internal chains of amylopectin and probably amylose [65,69–71]. Unexpectedly, the amorphous lamellae tend to be thicker in the absence of amylose (i.e., in waxy starches) than in its presence, whereas the crystalline lamellae are thinner [72]. The molecular density in the crystalline lamellae is lower in potato starch (1.10 gcm^{-3}) than in waxy maize (1.22 gcm^{-3}), probably due to the higher water content in the B-polymorph crystals, whereas the molecular density of the amorphous lamellae was found to be fairly similar in potato and waxy maize (0.52 and 0.46 gcm^{-3}, respectively, the latter being A-crystalline) [73]. Interestingly, only minor differences appeared to exist between waxy maize and normal maize, as well as between waxy maize and rice or cassava starch, all being A-type crystalline starches [73].

2.3. Granular Rings

The stacks of amorphous and crystalline lamellae form larger shells, or rings, being in the order of 100~400 nm thick (Figure 1) [74]. The rings are semi-crystalline in nature as they contain both the amorphous and the crystalline lamellae [66], but they have also been considered as "crystalline" [74] or "hard" [74,75] shells. The rings are embedded in an amorphous matrix [66] with a lower molecular density in potato (0.49 gcm^{-3}) than in waxy maize (0.68 gcm^{-3}) and other A-crystalline starches [73]. The matrix was described as an "amorphous background" [66], "semi-crystalline shell" [74], or "soft shell" [74,75]. The granular rings, often named "growth rings", are generally thinner at the periphery of the granules and thicker in their interior parts. In cereals (but not in potato [76,77]) the semi-crystalline rings has been considered as layers formed during photosynthesis in daylight, as old results had shown that the crystalline ring was formed only if the plant (wheat or barley) was grown under constant light supply [76,78]. Surprisingly, however, this could not be confirmed in a recent investigation, wherein the rings remained in barley starch grown under constant light [79]. In fact, the relative crystallinity decreased somewhat, instead of increased, in granules from constant light exposure. Around the granule's hilum, the rings might be absent and replaced by a void (filled with water, if the granule has not been dried) [80]. In some starch granules, especially in many cereals (e.g., maize, wheat, barley and sorghum), channels penetrate the granules from the surface [81–83]. Some of these channels even connect the surface to the interior voids, if present [29,80,84]. The channels are filled with proteins [25,29,83] and also phospholipids were found there [83]. The channels are important sites of penetration of different enzymes, such as α-amylases or glucoamylases, and diverse chemicals during modification of starch in vitro [85,86].

2.4. Blocklets

Scanning electron microscopy (SEM) and atomic force microscopy (AFM) have revealed protrusions, named blocklets, on the surface of the granules with sizes ranging approximately between 10~300 nm [74,87]. The size appears to be partly species specific. Potato granules have larger blocklets (50~300 nm) [88] than wheat granules (10~60 nm) [88,89]. Blocklets have also been observed within the growth rings in the interior parts of starch granules using diverse microscopic techniques and appear to transverse the entire rings (Figure 1) [74,90–95]. The exact nature of the blocklets remains unclear, however. Blocklets were clearly distinguished by AFM in dry, acid-treated potato starch, but upon in situ humidification blocklets in the semi-crystalline rings collapsed and simultaneously fused together [96], suggesting a flexible structure. It is known that the relative crystallinity in starch granules as measured by WAXS increases with the water content [97]. Moreover, the lamellar structure is also only identified in humidified granules by SAXS [98]. Thus, it appears that when blocklets fuse together, the crystalline structure simultaneously emerges. Blocklets have been found in both semi-crystalline and amorphous rings and Tang et al. [75] suggested the latter rings (or soft shells) consist of "defective" blocklets, in contrast to "normal" blocklets in the former, hard shells. The dimensions of the blocklets suggest that a single blocklet might represent a single, or a few, amylopectin molecules [75,90,94]. Also amylose might be a constituent of the blocklets and/or functioning as an interconnecting material outside the blocklets [75,99]. Park et al. [100] found that iodine-amylose complexes extend like "hairs" from blocklets on the granules' surface in potato and maize starches, and exclusively in maize also from gaps between the blocklets. This confirmed the "hairy billiard ball" hypothesis earlier proposed by Lineback [101]. Zobel [102], and later Saibene et al. [103], concluded that amylose interacts with amylopectin in potato starch granules, but not in maize. Possibly, this relates to how, or to which degree, amylose is involved in the blocklet structures.

3. The Major Starch Components

Any structural analysis of the starch component has to be preceded by the isolation of the starch components from the granules. The first step in this procedure is to dissolve the granules completely

in a solvent, most commonly 90% dimethyl sulphoxide (DMSO) followed by precipitation in ethanol, which results in a preparation known as "non-granular starch" [18]. Several methods have been used to further separate the amylose from the amylopectin, of which probably the most common is to precipitate the amylose as 1-butanol complex, a method developed by Schoch in 1942 [104]. In a frequently used modification of this method, Klucinec and Thompson [18] precipitated amylose in a mixture of 1-butanol and isoamyl alcohol and amylopectin was recovered from the supernatant after centrifugation. The precipitate was considered to contain a mixture of amylose and intermediate materials and, in the second step, this mixture was separated by precipitating amylose in 1-butanol only, whereas the intermediate material remained in the supernatant.

3.1. Amylose

3.1.1. Molecular Structure

Amylose is the minor, linear or slightly branched component of starch. Generally, branched amylose molecules are larger than their linear counterparts, however, the average chain lengths are shorter than the single chain in linear amylose [8,15,105–108]. The molecular size of amylose also varies between starches. Thus, potato amylose is among the largest so far reported, whereas cereal amyloses are smaller (Table 1) [109–112]. The proportion of branched amylose is estimated by degradation of the amylose molecules with the enzyme β-amylase. The linear component is completely transferred into maltose, whereas branched components only partly form maltose and the rest becomes a β-limit dextrin containing the internal part of the original molecule and all branches [106,113]. This showed that the proportion of branched amylose molecules varies among plants: The molar fraction of branched amylose in wheat, rice, and maize was 0.27, 0.31, and 0.44, respectively, whereas in sweet potato it was as high as 0.70 (Table 1) [8].

Table 1. Amylose content and structure in selected starches.

Source	Amylose (%)	DP_n [a]	CL_n [b]	β-LV (%) [c]	$N_{branched}$ (%) [d]	$NC_{branched}$ [e]
Wheat	17–34	980–1570	135–270	79–85	26–44	12.9–20.7
Rye	26–30	n.a. [f]	n.a.	n.a.	n.a.	n.a.
Triticale	23–27	n.a.	n.a.	n.a.	n.a.	n.a.
Barley	22–27	1220–1680	315–510	76–82	21–45	6.1–13.8
Oat	18–29	n.a.	592–907 [g]	n.a.	n.a.	n.a.
Rice	17–29	920–1110	230–370	73–87	31–69	5.7–9.7
Maize	20–28	960–830	305–340	81–84	44–48	5.3–5.4
Sorghum	22–30	n.a.	n.a.	n.a.	n.a.	n.a.
Sweet potato	19–20	3280	335	76	70	13.6
Potato	25–31	4920–6340	520–670	68–80	n.a.	n.a.

Note: Values represent a summary from the literature [6–8,13,33,62,63,101,102,109–111,113–131]. [a] Number average degree of polymerisation. [b] Number average chain length. [c] β-amylolysis limit value. [d] Molar fraction of branched amylose molecules. [e] Average number of chains in branched molecules. [f] Data not available. [g] Weight average values (CL_w).

Branched amyloses possess also short chains with lengths normally attributed to amylopectin (i.e., with DP < 100) [132]. The relative amount of these chains by weight is very low and often below the detection limit. On a number (molar) basis, however, these chains even predominate in the amylose. Hanashiro et al. [132] concluded that the organisation of the short chains in amylose is different from that in amylopectin, because their size-distribution is different from that generally found in amylopectin.

3.1.2. Amylose in the Granule

Even if amylose generally is considered to be in the amorphous state in the starch granules, the actual localisation of amylose within the granules remains a matter of debate. If starch granules

are treated in concentrated calcium chloride or lithium chloride solution, the granule erodes [133]. Some starches (e.g., potato and maize) erodes in a controlled manner starting from the surface inwards [134], and the solubilised matter as well as the remaining granular residues can be analysed [135]. Jane and co-workers [136,137] concluded that in both potato and maize starch granules the amylose is more concentrated at the peripheral parts of the granules than in their interior. In contrast, Blennow et al. [82,138], using confocal laser scanning microscopy and 8-amino-1,3,6-pyrenetrisulfonic acid (APTS) as a fluorescent probe for reducing ends, concluded that amylose is more confined to the interior parts of granules from potato, tapioca, maize, wheat, barley, and peas.

Another intriguing question is as to what extent amylose and amylopectin are associated with each other in the granule. When starch granules are heated in a water suspension, they swell to different degree depending on the temperature and amylose tends to leach out from the granules [139,140]. Amylose leaches more readily from maize starch granules than from potato starch granules. This, and many other experimental findings, led Zobel [102] to conclude that amylose in potato is associated with amylopectin, but not, or to a lesser degree, in maize starch granules, as well as other cereals such as rice and wheat. In contrast, Jane et al. [141] were able to cross-link amylose with amylopectin in the granules and came to the conclusion that amylose is interspersed among amylopectin molecules in both maize and potato granules.

With regards to the lamellar structure in the granules, amylose was shown to affect the SAXS analyses in wheat and, therefore, it was concluded that amylose together with amylopectin participates in the lamellar stacks [65]. Amylose introduces defects into the crystalline lamellae, which affects the stability of the crystals in the wheat starch granules [71,142,143]. This is also the case in rice and potato, and the involvement of amylose in the crystalline lamellae increases with amylose content in the granules [69,70,144].

3.1.3. Helical Conformation

An optimal solvent for amylose is concentrated DMSO, 6–8 M urea or 0.5 M KOH [145]. At pH > 13 the hydroxyl groups on the glucose residues become negatively charged and the molecule expands to its largest volume. In neutral water solution amylose obtains a random coil [146,147], an extended coil, a random coil with extended helical segments [148–150], or a wormlike helical conformation [151–153]—interpretation of experimental data are diverse. Nevertheless, amylose is unstable in aqueous solutions, especially in pure water, and forms double-helices that readily precipitate. These precipitates are crystallites of the B-polymorph type described above [154]. Single amylose molecules also form helices, which readily interact with a range of different compounds, such as iodine, fatty acids, or different alcohols to form inclusion complexes [155,156]. These left-handed helices are more compact than the double-helices and one turn of the helix may comprise between 6 and 8 glucosyl units depending on the guest molecule. Single amylose helices crystallises into so-called V-polymorph pattern [157,158]. WAXS powder diffractograms of many starch granules, especially from cereals, show a characteristic peak at 20° 2θ, which is attributed to V-amylose-phospholipid complexes [17,158–160]. However, it should be noted that a peak near 20° 2θ also is found in other than cereal starches with only low amylose content—even in amylose-free potato starch [44,160,161], and thus it can not solely be attributed to amylose-lipid complexes. Nevertheless, ^{13}C-cross-polarization/magic-angle spinning nuclear magnetic resonance (^{13}C CP/MAS NMR) studies confirmed that a part of the amylose in cereals is complexed with lysophospholipids [162]. Therefore, in cereals the amylose is divided into lipid-complexed amylose (LAM) and free amylose (FAM) [65,114]. The well-known blue colouration of starch with iodine is due to the amylose-iodine complex and is much used to quantitatively measure amylose in starch. However, LAM interferes with the measurement (in particular in cereal starches) and therefore only FAM is detected (corresponding to "apparent amylose", AAM). To achieve a measurement of the total amylose content (TAM), the sample has to be defatted completely [114]. LAM is then estimated as the difference between TAM and FAM.

3.2. Amylopectin

Amylopectin is the major, highly branched component in starch. The size of amylopectin is much larger than amylose. Physicochemical techniques, such as light scattering, viscometry or ultracentrifugation, suggest the weight average molecular weight (M_w) to be in the order of 10^7–10^8 Da [163–167], whereas number average values (M_n) are only 10^5–10^6 Da [7,111,168,169]. The polydispersity index (M_w/M_n) is therefore very large [170]. Takeda et al. [171] found that amylopectin from diverse sources consist of three size-fractions with approximate average DP_n-ranges of 700–2100, 4400–8400, and 13,400–26,500, of which the large molecules generally predominate.

3.2.1. Chain Categories

Amylopectin consists of numerous chains that are much shorter than the major chains found in amyloses. The size-distribution of the chains is analysed after debranching by either SEC [115,172–174], high-performance anion-exchange chromatography (HPAEC) [9,10,175] or fluorophore-assisted carbohydrate electrophoresis (FACE) [176–178] (Figure 2a). The chains of amylopectin are divided into two major groups, short (S) and long (L) chains; the division between the groups generally being at DP ~36. Short chains predominate and the molar ratio of S:L chains varies between starches, with cereals generally having the largest ratios (Table 2). As already mentioned, the S-chains form double helices that are involved in crystal formation in the starch granules [53]. S-chains are anchored on the L-chains, which thereby functions as the interconnecting chains and are mainly confined to the amorphous lamellae [11]. Already in 1952, Peat et al. [179] suggested a useful nomenclature of the chains in amylopectin: A-chains are unsubstituted, whereas B-chains are substituted with other chains, and the C-chain carries the single reducing-end group of the macromolecule but is otherwise similar to the B-chains. Hizukuri [180] found that the long B-chains (BL) could be further sub-divided into B2-chains (with average DP 42–48) and B3-chains (DP approx. 69–75) and eventually even longer chains. The major group of S-chains contains the A-chains and short B-chains (BS), the latter named B1-chains by Hizukuri [180]. In addition to S- and L-chains, several amylopectin molecules have also been found to contain extra long chains (EL-chains), sometimes called super-long chains [181]. EL-chains consist of several hundred or even thousand glycosyl units and thereby they resemble amylose chains and are difficult to distinguish from the amylose. They also form complexes with iodine resulting in overestimated amylose contents [182]. EL-chains were found in *indica* rice varieties, but not in *japonica* rice varieties [182], and also in, e.g., cassava, potato, barley, and wheat [109,183–187]. Finally, the C-chain in amylopectin preparations has generally a broad size-distribution between DP 15~120, with a peak around DP 40 [188]. As a single amylopectin molecule only contains a single C-chain, this shows that the length of the C-chain greatly varies between individual molecules.

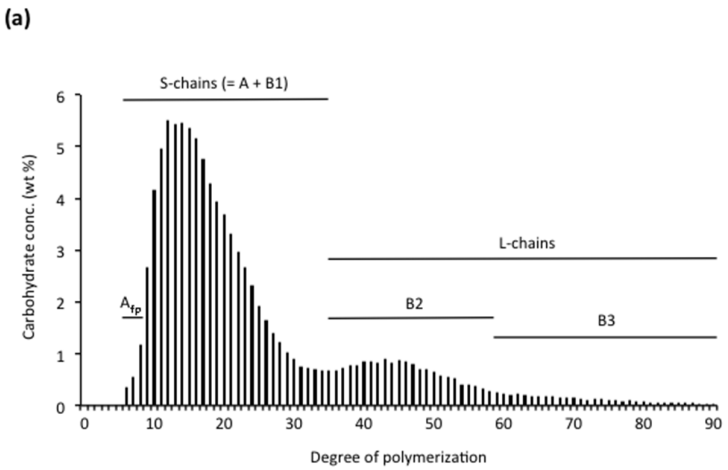

Figure 2. *Cont.*

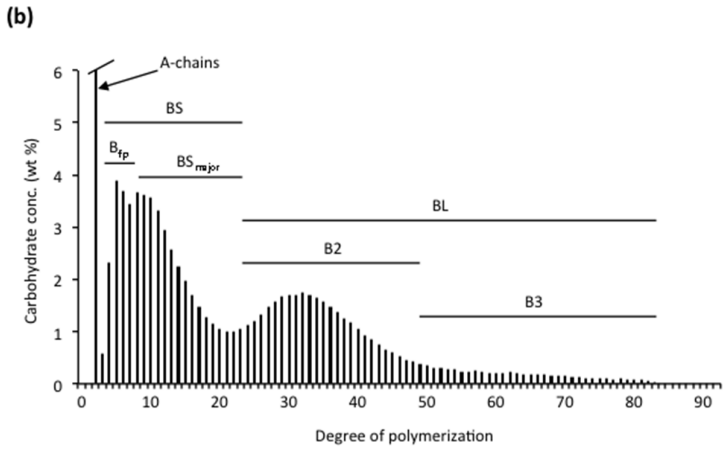

Figure 2. Unit chain profile of rice amylopectin (**a**) and its internal chain profile as obtained from the *φ*,β-limit dextrin (**b**), which possesses type 2 structure. Different chain categories are indicated. The A-chains (maltose peak) in (**b**) are actually external chain stubs and each B-chain carries a glucose residue as an external chain stub.

Table 2. Chain lengths and chain ratios in amylopectins [a].

Source	Structure [b]	CL	ECL	TICL	ICL	S:L	BS:BL	A:B
Wheat	A:1–2	17.7	12.3	12.7	4.4	16.2	6.8	1.4
Rye	A:1	17.4	10.7	12.6	5.3	16.2	7.3	1.1
Barley	A:1	17.6	11.5	12.3	5.1	17.9	8.6	1.0
Oat	A:1	17.0	10.7	12.6	5.3	18.2	8.6	1.0
Asian rice [c]	A:2	16.9	10.7	12.4	5.2	14.2	5.4	1.0
African rice [d]	A:2	18.1	12.1	11.9	5.0	11.7	5.0	1.0
Maize	A:2	19.7	13.1	12.6	5.6	9.9	6.3	1.1
Pearl Millet	A:2	18.0	12.0	11.9	5.0	15.9	7.4	1.0
Amaranth	A:2–3	17.7	11.4	13.4	5.3	10.0	4.2	1.1
Cassava	A:3	18.8	12.4	14.6	5.3	11.0	4.6	1.3
Potato	B:4	23.1	14.1	19.9	8.0	6.3	2.3	1.2

Note: Values represent a summary from the literature [9,189–194]. [a] CL = Number average chain length; ECL = External chain length; TICL = Total internal chain length; ICL = Internal chain length; S:L = Ratio of short to long chains; BS:BL = Ratio of short to long B-chains; A:B = Ratio of A- to B-chains. [b] Type of granular crystalline structure and type of amylopectin molecular structure. [c] *Oryza sativa*. [d] *Oryza glaberrima*.

External chains are defined as segments extending from the outermost branch of a chain to its non-reducing end [195]. By this definition, A-chains are completely external, whereas all B-chains have one external segment and the rest of the chain is internal. The whole internal chain from the outermost branch to the reducing-end side of the chain is called the total internal chain segment [196], whereas the chain was defined as a core chain segment if excluding the outermost branched residue [197]. Chain segments between branches are considered simply as internal chain segments [195] and the average length of these latter segments was the only internal parameter that could be measured before the invention of gel-permeation chromatography (Table 2).

It is necessary to remove the external chains in order to study the internal chain structure of amylopectin. There are two exo-acting amylolytic enzymes that can be used for this purpose. Phosphorylase *a* (the enzyme in muscles and liver involved in glycogen metabolism) removes successively one glucose residue from the non-reducing ends through a phosphorolytic mechanism producing glucose 1-phosphate [198,199], whereas β-amylase produces β-maltose by hydrolysis [200] (as mentioned above in Section 3.1.1). Neither of the enzymes by-pass the branches. Phosphorylase *a* produces a *φ*-limit dextrin (*φ*-LD), in which all A-chains have been reduced into maltotetraosyl stubs [201–203]. If the *φ*-LD is further hydrolysed with β-amylase, each chain is reduced by an additional maltose residue, thus leaving the A-chains as maltosyl stubs in the so-called *φ*,β-LD [202].

In the β-LD the length of external residues depends on if the original external segment contains an odd or even number of glucosyl units. Therefore, A-chains remain as DP 2 or 3 [204].

The internal chains are analysed after debranching with isoamylase and/or pullulanase (Figure 2b). It should be noted that there are some differences in the preferences for different substrates by the two enzymes: pullulanase (which completely hydrolyses the polysaccharide pullulan) more effectively hydrolyses maltosyl chain stubs, whereas isoamylase (which possesses no activity against pullulan) more effectively hydrolyses whole amylopectin [205–208]. Glucosyl branch-stubs are resistant to both enzymes [209]. The ratio of A:B-chains is normally between 1.0 and 1.4 (Table 2). The internal short B-chains (BS) in the internal chain profiles are distinguished as two sub-groups: "fingerprint" B-chains (B_{fp}) possessing a typical "fingerprint" profile in the chromatograms depending on the plant source, and a major group of BS-chains (BS_{major}) [9]. The internal BL-chains are divided into the same sub-groups (B2- and B3-chains) as for the unit chains in the original amylopectin. In the internal chain profile they are shorter, however, as the external segment has been removed so that the division between BS- and BL-chains typically is between DP 23 and 28, depending on the plant source (Figure 2b) [9]. Also the A-chains have been sub-divided into two groups. The shortest chains in the unit chain profile of the whole amylopectin (before removing the external chains, Figure 2a) at DP 6–8 are considered as A-chains (they are likely too short to be B-chains) and have been called "fingerprint" A_{fp}-chains in analogy to internal B_{fp}-chains because of their typical profiles in the chromatograms [203]. The rest of the A-chains were considered to be crystalline A-chains ($A_{crystal}$) [189] as it was shown that chains with DP < 9 do not readily form double-helices with other chains [210].

The unit chain profile of the whole amylopectin can be used for the estimation of the average chain length (CL). By combining the information from both the unit and internal chain profiles, the average external, total internal, and internal chain lengths (ECL, TICL, and ICL, respectively) can also be calculated (Table 2) [202,203].

3.2.2. Structural Types

The internal chain profile of amylopectin was found to be specific for different plant species and was divided into four types suggesting distinctive structural groups [9]. Type 1 amylopectin is typical for certain cereals, namely barley, rye and oat. In these starches the relative number of long chains is very small with hardly any B3-chains (typically < 1%). The ratio of S:L-chains (as well as BS:BL) is therefore high (Table 2). The BS-chains possess an unusually broad size-distribution due to an abundance of BS_{major}-chains resulting in an almost complete disappearance of the otherwise typical groove between BS- and BL-chains. Type 2 amylopectin has more B-chains than type 1, and less BS_{major}-chains and therefore the groove between BS- and BL-chains is clearly distinguished (Figure 2b). In addition, B_{fp}-chains are more abundant than in most other structural types. The important cereals maize and rice [9,190], as well as the pseudo-cereal amaranth [211], belong to type 2 amylopectin, whereas wheat amylopectin was found to have an internal chain structure intermediate to that of types 1 and 2 [212]. Type 3 amylopectin, which includes e.g., cassava and mung bean starch, has less B_{fp}-chains than types 1 and 2 and slightly elevated B3-chains. Finally, type 4 amylopectin, which includes all B-crystalline starches (e.g., potato and edible canna), possesses the highest amount of B3-chains and thus the lowest S:L chain ratio (Table 2) [9].

3.2.3. Branched Units

The chains in amylopectin are arranged into larger or smaller groups and diverse groups can be isolated using endo-acting enzymes. Though there exist a manifold of endo-acting amylolytic enzymes, only few have been used for structural analyses. As the α-amylase of *Bacillus amyloliquefaciens* is the enzyme that by far has been mostly used for the purpose of investigating branched structural parts of diverse amylopectins, this review only considers the results obtained by this particular enzyme. Among several amylolytic enzymes, *B. amyloliquefaciens* α-amylase gives the most pronounced endo-action pattern [213] and is therefore especially useful for the isolation of larger branched

α-dextrins from amylopectin. The enzyme contains nine subsites arranged around the catalytic site [214,215]. The reaction is effective only with all subsites filled with glucosyl units of the substrate. Initially the rate of the reaction is very fast because at this stage the substrate contains several long internal chain segments that completely fill up the subsites [214]. Soon, however, this criterion is no longer fulfilled, resulting in a quite dramatic decrease in the reaction rate. α-Dextrins isolated at this stage are considered to represent unit clusters of chains [216–222]. Because of the nature of the subunits in the enzyme, the internal chain segments between branches in the isolated clusters is DP < 9, and this is the only structural definition of a cluster so far presented [223]. Groups of clusters, named "domains", have also been isolated by interrupting the hydrolysis before the fast, initial stage ends [211,224–226].

As the α-amylase also attacks the external chains in amylopectin in a more uncontrolled fashion, the remaining external segments have diverse lengths [227,228] and are removed by the addition of phosphorylase and/or β-amylase. The limit dextrins of the clusters or domains can then be structurally characterised. The size-distribution of clusters is large, varying from approximately DP 15 up to DP 500 or more, and depends on the source of the amylopectin [224,227–229]. The largest clusters are found in type 1 and 2 amylopectins, which include the cereals, having average size around DP 66–73 [229]. This corresponds to an average number of chains (NC) of about 11–14. However, barley was found to have very large clusters with NC 19.5 (Table 3). In the isolated dextrins, the amount of long chains have been reduced compared to the original amylopectin, in clusters more than in domains, showing that the α-amylase attacks the long internal chains [224,226–228]. As a result, new shorter chains are formed, some of which are similar to those already existing in the amylopectin, others apparently representing new categories, which is especially significant around the characteristic groove in the chromatograms between short and long chains of amylopectin. The chains in the α-amylolysis products were therefore assigned lower case letters to emphasise their difference from chains in amylopectin (assigned capital letters) [229].

The apparent clusters isolated from amylopectins are very slowly hydrolysed further by the α-amylase eventually into small α-LDs, which constitute the ultimate branched units called building blocks [224,230]. The molecular composition and the detailed structure of building blocks is very complex. Nevertheless, the concept of building blocks can be rationalised to consist of diverse groups of α-LDs with increasing number of chains. Thus, group 2 consists of building blocks with two chains and have DP 5–9, group 3 have three chains (DP 10–14) and group 4 have four chains (DP 15–19) [231–233]. As the complexity of each group increases with the size, the larger building blocks have only been isolated as course preparations. Therefore, group 5 consists of dextrins with between 5~7 chains (average 6 chains) and group 6 have at average ~10 chains and DP > 35 [233]. The chains in the building blocks are very short: besides a-chains (DP 2 and some at DP 3), most b-chains are concentrated around DP 5–6. In the larger building blocks trace amounts of chains with DP 12~15 can be detected [233]. In all samples analysed so far, group 2 building blocks predominate in the clusters: roughly 40–65% of all building blocks (on a number basis) have only two chains. The abundance then decreases with increasing number of chains, so that group 6 only represents a few per cent or less of the blocks, and the size-distribution is surprisingly similar regardless the structural type of amylopectin (Table 3) [191,211,223,229–232,234–237].

Table 3. Structure of intermediate α-dextrins ("clusters") isolated from amylopectin with the α-amylase of *B. amyloliquefaciens* [a].

Source	Structure [b]	NC	CL	TICL	ICL	IB-CL	NBbl	Molar Distribution of Building Blocks (%) [c]				
								2	3	4	5	6
Wheat	A:1–2	14.2	5.8	11.9	3.6	6.4	6.3	57	24	10	8	1
Rye	A:1	11.5	6.1	10.5	4.0	5.9	5.5	55	28	9	7	1
Barley	A:1	19.5	6.3	10.0	4.0	6.0	10.4	65	25	5	4	1
Oat	A:1	11.8	6.1	10.4	4.1	5.7	5.7	55	27	9	7	2
Asian rice [d]	A:2	12.0	6.8	7.9	4.7	6.9	5.7	50	29	11	9	1

Table 3. *Cont.*

Source	Structure [b]	NC	CL	TICL	ICL	IB-CL	NBbl	Molar Distribution of Building Blocks (%) [c]				
								2	3	4	5	6
African rice [e]	A:2	14.1	5.9	7.9	3.8	6.5	5.1	40	29	13	14	4
Maize	A:2	12.5	5.4	10.5	3.3	6.2	4.2	51	27	10	12 [f]	
Amaranth	A:2–3	8.8	6.4	10.3	4.5	6.8	4.2	55	29	8	8 [f]	
Cassava	A:3	10.0	7.0	12.0	4.6	7.1	5.1	59	30	5	6 [f]	
Waxy potato	B:4	6.2	7.9	12.4	5.4	8.0	3.1	48	31	13	8 [f]	

Note: Values represent a summary from the literature [191,211,223,225,227,229,232,234,236,238]. [a] NC = Average number of chains in the cluster; CL = Number average chain length; TICL = Total internal chain length; ICL = Internal chain length; IB-CL = Inter-block chain length; NBbl = Average number of building blocks in the cluster. [b] Type of granular crystalline structure and type of amylopectin molecular structure. [c] Building blocks of group 2 have two chains, group 3 have three chains, group 4 have four chains, group 5 have 5~7 chains, group 6 have > 7 chains. [d] *Oryza sativa*. [e] *Oryza glaberrima*. [f] Group 5 + 6.

It is noted that the largest building blocks in group 6 contains as many chains as is found in a large part of the clusters. However, the chains in the building blocks are much shorter and the density of branches (DB) is higher (14~20%) [211,229,234,235,239] than in clusters (11~15%) [211,225,229,230,234,239] due to very short distances between the branches: ICL is only 1.4~2.3. The large clusters in cereals have typically 4–6 building blocks, whereas small clusters (many roots and tubers) contain 3~5 blocks on average (Table 3) [229]. Interestingly, the average chain length between the building blocks (the inter-block CL, IB-CL) increases successively in clusters from type 1 to type 4 amylopectins from IB-CL ~5.7 to 8.0 [229]. In only few cases so far the inter-cluster CL (IC-CL) has been estimated in isolated domains from amylopectins. IC-CL appears mostly to be between 10~20 [211,225–227,231]. The shortest IC-CL (9.5) was estimated in sweetpotato [226] and barley [231] and the longest (IC-CL 27) in a domain of waxy potato [227]. IB-CL was shown to correlate positively with the onset gelatinisation temperature when starches from ten diverse sources were compared [240]. This remarkable finding suggests that the inter-block segments, and most probably also the inter-cluster segments, have a key role when it comes to contributions to the thermal properties of starch granules.

It is the b-chains in the clusters that interconnect the building blocks, i.e., they consist of inter-block segments as well as intra-block chain segments. The b-chain is given a number that corresponds to the number of inter-block segments along the chain (Figure 3) [229]. Thus, b0-chains lack inter-block segments, because they are found completely inside the building block. The DP of these chains is 3–6 and, if not formed by the α-amylase, they correspond to B_{fp}-chains in the original amylopectin. b1-chains contain one inter-block segment. They have DP 7–18, and were sub-divided into b1a-chains (DP 7–10), which practically lack an internal segment at the reducing-end side of the chain, and b1b-chains (DP 11–18), which have a segment at the reducing-end side with maybe up to six glucosyl units that extends through an internal building block. b2-chains (DP 19–27) have two inter-block segments and segments that extend through building blocks. Finally, b3-chains (DP $\geq$ 28) have at least three inter-block segments [229]. Roughly, one can consider that each building block on a b-chain contributes with an intra-block segment (DP 5~6) in addition to an inter-block segment (DP 5~8) that connects to the next block, i.e., the b-chains theoretically possess a periodicity of around 12 residues.

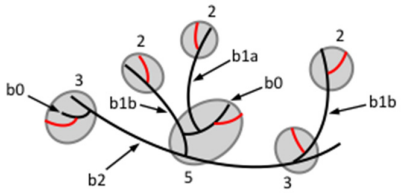

Figure 3. Chain types and building blocks in an isolated typical "cluster". a-Chains are shown in red and b-chains (**black**) are numbered based on the number of inter-block segments they are involved in. Building blocks are encircled (**grey**) and numbered according to the number of chains they contain.

3.2.4. Organisation of Structural Units in Amylopectin

The challenge in understanding the structure of amylopectin is to organize the pieces of information (in the form of unit chains, internal chains, and diverse branched units with their composition of chains) into a meaningful model of the entire macromolecule. Besides fitting with the experimental data, any model must also fit with the present knowledge of the granular structure and, importantly, it shall be useful in explaining the properties of starch. Moreover, any model must also agree with what has been achieved in the field of starch biosynthesis, or eventually even boost or refine the present understanding of starch biosynthesis (see review of starch biosynthesis by Tetlow and Emes in this Special Issue). Several models of amylopectin structure have been suggested through the years, and historically their development follows the development of new techniques and the discoveries of new enzymes useful for structural studies [241]. In this review two models are described, namely the "cluster model" and the "building block backbone model", of which the former is most widely accepted today, but the latter is the most recent model based on experimental results previously not available.

The cluster model was originally proposed in 1969 by Nikuni [242] and independently by French in 1972 [45]. In this model, the short chains in amylopectin form clusters and the long chains interconnect the clusters (Figure 4a). The model is based primarily on the following findings: (i) Acid treatment of starch granules removes mostly the amorphous parts, whereas the crystalline parts remain largely intact. Size-distribution analyses of the molecules in the remaining granular residues (commonly named "lintners" if the granules are treated in dilute HCl, or "Nägeli amylodextrins" if they are treated in dilute H_2SO_4) show that most of the branches have been removed and the major part of the dextrins are linear chains with DP 13~16 [17,47,49,51,243]. The result suggests that the branches are mostly confined to the amorphous parts and connects to the short chains in the crystalline parts. (ii) The periodic length of 9–10 nm revealed by SAXS corresponds to one amorphous and one crystalline lamella [66], in which the thickness of the latter closely match the DP of the short chains in the acid-treated starch [69,142,143]. (iii) Gel-permeation chromatography shows that amylopectin consists of two major groups of chains (S- and L-chains) [244]. (iv) The polarization cross in starch granules shows that the molecules are arranged radially with all chains pointing in the same direction toward the surface of the granules [45].

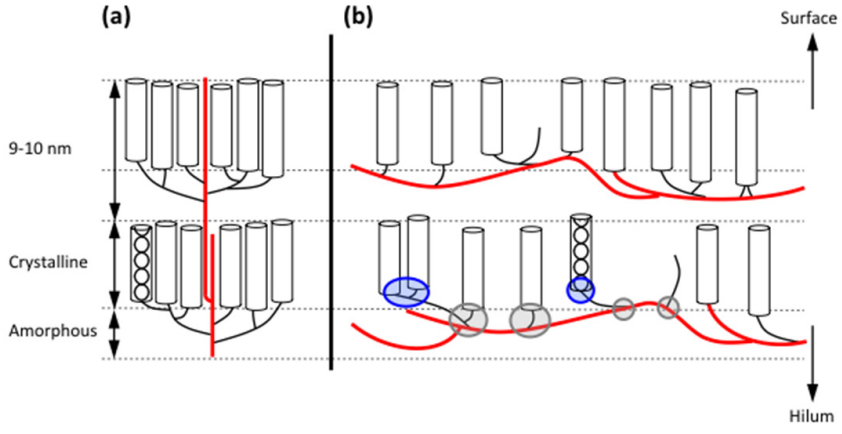

Figure 4. Amylopectin in the semi-crystalline growth ring depicted based on the cluster model (**a**) or the building block backbone model (**b**). The crystalline and amorphous lamellae are indicated by dotted grey lines. Long B-chains (thick red lines) and short chains (black lines) are shown. The backbone in (**b**) carries internal building blocks (some encircled in grey) and can also carry short BS_{major}-chains that form branches to the backbone and connect to external building blocks (encircled in blue). Cylinders symbolise double-helices formed by external chains. Single chains introduce defects in the crystalline lattice. The directions toward the surface and the hilum of the granule are indicated at the right.

The works by Robin et al. [46] and Manners and Matheson [245] were also in favour of the cluster model. Moreover, multiply branched dextrins formed from amylopectin using cyclodextrin glycosyltransferase from *Klebsiella pneumoniae* [246], a maltotetraosyl forming enzyme from *Pseudomonas stutzeri* [247], or α-amylases from barley [248] and *Bacillus subtilis* [216], suggested these dextrins were the clusters in amylopectin. Hizukuri [180] found a periodicity in chain length of 27–28 glucosyl units among the B-chains of amylopectin, which closely corresponds to the periodic length of 9–10 nm, i.e., the length of a chain in the form of a double-helix with 6 residues per turn and a pitch of 2.1 nm. Hizukuri [180] therefore suggested that B2-chains span two clusters and B3-chains span three clusters, etc.

Later results have challenged the accuracy of the cluster model, however. By comparing the unit chain profiles of a range of amylopectins, Hanashiro et al. [10] found a periodicity in chain length of 12 glucose residues among the S-chains, but not among the L-chains. This shorter periodicity among S-chains, and the lack of a periodicity among L-chains, cannot be explained as B-chains penetrating successive layers of clusters. Instead, it appears that the periodicity of 12 residues stems from the interconnection of building blocks in the isolated α-dextrins as explained above. O'Sullivan and Pérez [249], working with molecular modelling, showed that the amorphous chain segments involved in interconnecting double-helices in the crystalline lamellae into parallel alignment (to match with either the A- or B-polymorph) take diverse and almost perpendicular directions to the helices. Therefore, it is most unlikely that L-chains penetrating the crystalline lamella as radially organised double-helices also extend through the amorphous lamella as helices and in the same radial direction. Bertoft and co-workers [225,229,230,232] found that the structure of the multiply branched dextrins produced by α-amylase from *B. amyloliquefaciens* does not conform to the expected structure of clusters proposed in the cluster model. The model predicts that isolated clusters only contain short chains, because the long chains have to be cleaved in order to release the clusters from the macromolecule. However, the isolated dextrins still contain some long chains, even if the L-chains are reduced in number compared to the original amylopectin. Indeed, an aggravating circumstance is that the smaller the isolated apparent clusters are, the more long chains they tend to contain. Furthermore, the S:L chain ratio of amylopectin predicts the average number of chains (NC) in isolated clusters from a certain starch sample, but the isolated α-dextrins most often have lower NC than the predicted theoretical value [229]. Only in the case of amylopectins with type 4 internal structure (the B-crystalline starches), NC of isolated clusters agrees with the cluster model. These circumstances led to a need to find a model that better matches experimental data and resulted in what is now known as the building block backbone model [250].

In the building block backbone model, the L-chains (or BL-chains) in amylopectin are linked to each other and form collectively a longer backbone (Figure 4b). Building blocks are outspread along the backbone and form an integrated part (these blocks are characterised as "internal") [250]. Building blocks of all kinds are completely randomly distributed along the backbone [251]. In some amylopectins, notably those with type 1 structure, some of the longer BS-chains are likely also involved in the backbone [229]. BS-chains probably also form shorter branches to the backbone, which connect to building blocks outside the actual backbone ("external" building blocks) [250], but some starches might also have longer branches extending from the backbone [229]. The short chains (S-chains) extend from the building blocks in a more or less perpendicular direction. In the starch granules, the S-chains form the double helices of the crystalline lamellae, i.e., exactly as in the cluster model (Figure 4). In contrast to the cluster model, however, the backbone is (more or less) completely embedded in the amorphous lamella and extends along it, rather than traversing the stacks of lamellae in the semi-crystalline "growth ring". The building blocks are separated by inter-block segments (DP 5–8 depending on starch source, Table 3) and occasionally these segments are slightly longer, forming the inter-cluster segments that the α-amylase of *B. amyloliquefaciens* readily attacks at initial stages of hydrolysis [225,232]. It is apparent, however, that the actual function of the inter-cluster segments is the same as that of the inter-block segments; they interconnect building blocks. Therefore, *the branched*

structural units in the model are the building blocks, and the reader may already have noticed that clusters in the traditional meaning do not exist in the backbone model.

The α-dextrins that the α-amylase produces at early stages of hydrolysis are therefore only *apparent* clusters, which are formed due to the preferential attack at inter-block segments with DP ≥ 9. This explains why the structure of the α-dextrins does not correspond to the clusters of the cluster model. Instead, the backbone model explains the fact that some dextrins still contain long chains, because the long chains are not involved in the interconnection of any clusters (as there exist no clusters). The long chains are instead involved in interconnecting building blocks and, depending on the random placement of long inter-block segments, the released dextrins will contain a variable number of building blocks, inter-block segments and chain lengths, some of which corresponds to the long b3-chains [229]. This also explains the very broad size-distribution of the α-dextrins. As the sequence of types of building blocks along the backbone is random, the length of both the intra- and inter-block segments along the backbone varies randomly [251], and therefore there is no apparent periodicity in chain length among the L-chains. This explains why Hanashiro et al. [10] did not find a periodicity of DP 12 at DP > 36. Among the shorter chains (b2- and b1-chains in α-dextrins) there is a periodicity, however, because these chains are mostly found as short side-chains to the backbone and have well defined IB-CL. The backbone model also explains the fact that the ratio of S:L chains in amylopectin generally does not correlate with the NC of the isolated *apparent* clusters, because the L-chains have a different function in this model compared to the cluster model.

3.2.5. Possible Implications of the Backbone Structure on Starch Properties and Biosynthesis

It is envisioned that the organisation of the amylopectin molecules in the layers of lamellae in the starch granules is rather random in the sense that the backbone possibly extends in any direction and, moreover, it is possibly far from having a straight, extended conformation. In fact, backbones from individual molecules might even cross each other, forming an intricate network [252]. The double-helices extend from this network into the crystalline lamella. This then suggests that double-helices from individual molecules come close together and crystallize into either the A- or B-polymorphic pattern. It was noted above that the dimensions of the nano-crystals, that have been isolated by mild acid hydrolysis of starch granules and stems from the crystalline lamellae [67], are so large so that more than hundred double-helices contribute to the individual crystals [68]. A network of backbones in the amorphous lamella will thus contribute with double-helices to form the crystallites in a cooperative fashion, which explains the dimensions of the isolated nano-crystals. It is also interesting to notice that O'Sullivan and Pérez [249] showed that only very limited combinations of internal chain lengths result in parallel alignment between two adjacent double-helices found in the same macromolecule. In fact, the combinations are so few that it is very unlikely that double-helices from a single cluster, as suggested in the cluster model, could contribute to any crystalline structure. In other words: clusters are not needed for formation of the crystalline lamellae. On the contrary, they would likely prevent their formation by being too tightly branched (which is how they mostly are depicted). Interestingly, it has been shown that debranching enzymes are needed for accurate formation of the semi-crystalline starch granules. Without the debranching activity during biosynthesis, amylopectin is not "trimmed", resulting in a too dense branching pattern and the formation of water-soluble phytoglycogen [253]. Unlike the cluster model, the building block backbone model has a comparatively open structure: As noted above, the most common building block, representing about 50% of all blocks and about 25% of all branches [230], has only two chains and one branch. Both sides of this single branch are occupied by inter-block (or inter-cluster) segments (IB-CL 5–8, or more). This open structure might be a result of the "trimming" activity of debranching enzymes and suggests a flexible structure, in which the rather long segment can move and bend quite freely, in contrast to the tightly branched clusters in the cluster model, resulting in the ordered A- or B-crystallites. When, in addition, these flexible segments are part of the intricate network in the amorphous lamellae, it is easy to understand the extreme swelling that starch granules possess in warm aqueous solution [90,254–258].

Once the double-helical order in the crystalline lamellae collapses (the polarization cross disappears) due to water uptake into the granules, which exercises an increasing pressure on the crystallites, nothing prevents the granules from swelling. However, the granule integrity remains intact because the backbones of the amylopectin molecules stretch in all directions (compare with a balloon) and, only when they loose contact with each other the granules disintegrate [252]. In the presence of amylose, starch granules are more stable than waxy granules [161,259,260]. The stabilising effect is possibly due to amylose intermixed with amylopectin backbones in the amorphous lamellae [203], which decreases their flexibility and retards the swelling. Amylose can also transverse the stacks of lamellae [69–71], acting like a "glue" between the lamellae, which has a similar effect.

Donald and co-workers have suggested that amylopectin behaves like a side-chain liquid-crystal [98,261–263]. This model suggests that the double-helices are linked to the amorphous "backbone" of clusters through flexible spacer arms. The flexibility of the spacer arms explains phenomena like annealing and gelatinisation. With the exception of clusters, their model, in fact, resembles the building block backbone structure. In the latter, the inter-block segments represent the flexible arms. The longer the segments, the better the flexibility. Indeed, Vamadevan et al. [240,264] showed that both annealing and the onset gelatinisation temperature positively correlate with IB-CL. Another indication of the nature of the backbone is the interaction of the β-limit dextrin of amylopectin with iodine, which gives rise to a faint colour at low wavelengths (λ_{max} is about 507~540 nm) [96,265,266]. As the β-LD lacks external chains, the result shows that the backbone possesses segments long enough to interact with iodine, i.e., these segments, which presumably are longer inter-block segments, form single-helices and inclusion complexes with iodine. The exact nature of these segments is not clarified, however. It is interesting to notice that also starch granules form complexes with iodine, which suggests that the molecular components in the granules possess segments flexible enough to form the helices. Amylose-containing granules stain dark blue due to the complex with amylose [159,267]. Notably, these iodine-treated granules possess very restricted swelling and amylose leaching [140,257,268]. However, also amylopectin interacts, as shown by the fact that amylose-free granules stain red [267]. As the majority of the short chains are engaged in double-helix formation inside crystallites (and probably also are too short to give a notable colour) it is possible that the amorphous backbone is involved in the interaction. Indeed, this is even more remarkable as the backbone will hardly be able to turn into a helix when the short chains are fixed into their positions in the crystals. Therefore, it is suggested that the helix pre-exists and iodine either simply enter its central cavity, or the helix exists in a more extended conformation that contracts when the iodine binds. Tiny differences in the WAXS diffraction pattern of iodine-stained starch granules have been reported [159,160,269], which suggests that some movements happens and are reflected in the packing of the double-helices in the crystallites.

A helical structure of the backbone also opens new implications for the structure of the double-helices formed by the short chains in amylopectin. Hitherto most, if not all, focus has been on double-helices formed by an A- and a B-chain (Figure 5a). It was shown that these helices are stabilised by the branch point between the two chains [53]. Other possible combinations could, however, be between two A- or two B-chains [250], if they are close enough to each other such as in a building block. As already discussed, however, about half of the building blocks consist only of two chains (one a- and one b-chain). In external blocks, the well-established A-B helix should then be formed [250]. However, in internal blocks the b-chain is a part of the backbone and the a-chain is single. If the inter-block segment between two such building blocks is helical (note that many IB-CL are ~6, i.e., a helical turn), the two A-chains will be adjacent in space and could interact to form a double-helix (Figure 5b) [230,250]. One might expect a comparatively weak double-helix in this case as the stabilising branch is absent.

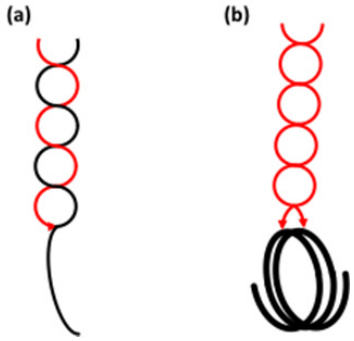

Figure 5. Detail of the backbone model suggesting the formation of double-helices. (**a**) A-B double-helix in an external building block formed by an A-chain (**red**) and the external segment of a B-chain (**black**). (**b**) A-A double helix formed by two A-chains connected to a helical backbone (bold black line). Arrows symbolise branches.

If the backbone partly (or completely) exists as a pre-helical structure, it may also retain this conformation in solution. In fact, indications in this direction have been observed. It was found that the gel-forming properties within a series of four waxy rice starches greatly varied [265]. Structurally, the only differences found were tiny differences in the internal chain lengths, whereas the external chain lengths were similar. It was therefore concluded that the small differences in internal structure were the reason for the different rheological properties. Possibly, external chains in one molecule could interact with single-helical internal segments in the other molecules, likely by forming double-helices [265].

It is obvious that the building block backbone model exerts challenges on our view of the biosynthesis of amylopectin—and from there the entire starch granule. One important enzyme in the synthesis of amylopectin is starch branching enzyme (SBE) [270]. The remarkable action of SBE is threefold: (i) the enzyme hydrolyses a (1,4)-linkage in one chain, (ii) it transfers the released non-reducing end-side of the cleaved chain segment to another chain (or eventually the same chain), and (iii) it attaches the chain segment to the other chain by synthesising a (1,6)-linkage. It was shown that SBE prefers double-helices rather than single chains as substrate [271]. In the light of the backbone possibly having a single-helical structure, it is tempting to suggest that the backbone is synthesised from a double-helical "pre-backbone". The result of the action of SBE on a double-helical substrate was, in fact, discussed by Borovsky et al. [271] already in 1979 and is presented in Figure 6. In their work, they suggested that the transfer reaction after the cleavage of the first chain simply involves a transfer to the other strand of the double-helix (a distance less than 10.5 Å, which is the approximate diameter of the double-helix). Continuous enzyme action results in an extensively branched backbone, with some branches forming building blocks (A- and B_{fp}-chains) or shorter branches (BS_{major}-chains) to the backbone, others being branches in the backbone itself (mostly BL-chains).

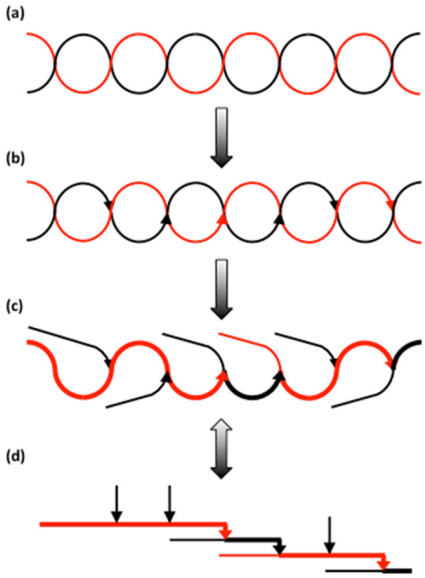

Figure 6. Possible formation of the backbone from a double-helix precursor based on the suggestion by Borovsky et al. [271]. (**a**) A double-helix formed by two polyglucan chains (black and red). (**b**) Branches (arrows) inserted in the double-helix by starch branching enzyme. (**c**) The same structure as in (**b**) but with the external chains (thin lines) extending out from the former double-helix. The chain segments forming a backbone are shown as bold lines. (**d**) The same structure as in (**c**) drawn as a laminated amylopectin model originally proposed by Haworth et al. in 1937 [272].

4. Conclusions

Starch granules consist of several structural levels, starting from their size and morphology going through their internal structures, such as growth rings, blocklets, and crystalline and amorphous lamellae, down to the double-helical arrangement of the external chains of amylopectin, spanning a size-range from micrometres to Ångströms. Whereas the exact involvement of the minor, mainly linear component amylose in the granules remains uncertain, the branched, major component amylopectin is generally agreed to be the principal contributor to the semi-crystalline structure of the granules. As opposed to the more traditional cluster model, the building block backbone model of amylopectin is based on new findings obtained directly on α-dextrins isolated from amylopectin. These dextrins, first believed to be clusters in the traditional meaning, later turned out not to be compatible with the cluster model, but have instead resulted in the new structural concept. In addition, the building block backbone model is compatible with all the former data spoken in favour of the cluster model and it explains satisfactorily many of the properties of starch granules. Moreover, in addition, it implies new ways to look upon the biosynthesis of starch.

References

1. Jane, J.-L.; Kasemsuwan, T.; Leas, S.; Zobel, H.; Robyt, J.F. Anthology of starch granule morphology by scanning electron microscopy. *Starch/Stärke* **1994**, *46*, 121–129. [CrossRef]
2. Geera, B.P.; Nelson, J.E.; Souza, E.; Huber, K.C. Composition and properties of A- and B-type starch granules pf wild-type, partial waxy, and waxy soft wheat. *Cereal Chem.* **2006**, *83*, 551–557. [CrossRef]
3. Evers, A.D.; Greenwood, C.T.; Muir, D.D.; Venables, C. Studies on the biosynthesis of starch granules. Part 8. A comparison of the properties of the small and the large granules in mature cereal starches. *Starch/Stärke* **1974**, *26*, 42–46. [CrossRef]
4. Morrison, W.R.; Gadan, H. The amylose and lipid contents of starch granules in developing wheat endosperm. *J. Cereal Sci.* **1987**, *5*, 263–275. [CrossRef]

5. Mäkelä, M.J.; Korpela, T.; Laakso, S. Studies of starch size and distribution in 33 barley varieties with a celloscope. *Starch/Stärke* **1982**, *34*, 329–334. [CrossRef]
6. Hizukuri, S.; Takeda, Y.; Yasuda, M.; Suzuki, A. Multi-branched nature of amylose and the action of de-branching enzymes. *Carbohydr. Res.* **1981**, *94*, 205–213. [CrossRef]
7. Hizukuri, S.; Takeda, Y.; Maruta, N.; Juliano, B.O. Molecular structure of rice starch. *Carbohydr. Res.* **1989**, *189*, 227–235. [CrossRef]
8. Takeda, Y.; Hizukuri, S.; Takeda, C.; Suzuki, A. Structures of branched molecules of amyloses of various origins, and molecular fractions of branched and unbranched molecules. *Carbohydr. Res.* **1987**, *165*, 139–145. [CrossRef]
9. Bertoft, E.; Piyachomkwan, K.; Chatakanonda, P.; Sriroth, K. Internal unit chain composition in amylopectins. *Carbohydr. Polym.* **2008**, *74*, 527–543. [CrossRef]
10. Hanashiro, I.; Abe, J.-I.; Hizukuri, S. A periodic distribution of chain length of amylopectin as revealed by high-performance anion-exchange chromatography. *Carbohydr. Res.* **1996**, *283*, 151–159. [CrossRef]
11. Imberty, A.; Buléon, A.; Tran, V.; Pérez, S. Recent advances in knowledge of starch structure. *Starch/Stärke* **1991**, *43*, 375–384. [CrossRef]
12. Colonna, P.; Mercier, C. Gelatinization and melting of maize and pea starches with normal and high-amylose genotypes. *Phytochemistry* **1985**, *24*, 1667–1674. [CrossRef]
13. Gérard, C.; Barron, C.; Colonna, P.; Planchot, V. Amylose determination in genetically modified starches. *Carbohydr. Polym.* **2001**, *44*, 19–27. [CrossRef]
14. Shi, Y.-C.; Capitani, T.; Trzasko, P.; Jeffcoat, R. Molecular structure of a low-amylopectin starch and other high-amylose maize starches. *J. Cereal Sci.* **1998**, *27*, 289–299. [CrossRef]
15. Yoshimoto, Y.; Tashiro, J.; Takenouchi, T.; Takeda, Y. Molecular structure and some physicochemical properties of high-amylose barley starches. *Cereal Chem.* **2000**, *77*, 279–285. [CrossRef]
16. Carciofi, M.; Blennow, A.; Jensen, S.L.; Shaik, S.S.; Henriksen, A.; Buléon, A.; Holm, P.B.; Hebelstrup, K.H. Concerted suppression of all starch branching enzyme genes in barley produces amylose-only starch granules. *BMC Plant Biol.* **2012**, *12*, 223–238. [CrossRef] [PubMed]
17. Gérard, C.; Colonna, P.; Buléon, A.; Planchot, V. Order in maize mutant starches revealed by mild acid hydolysis. *Carbohydr. Polym.* **2002**, *48*, 131–141. [CrossRef]
18. Klucinec, J.D.; Thompson, D.B. Fractionation of high-amylose maize starches by differential alcohol precipitation and chromatography of the fractions. *Cereal Chem.* **1998**, *75*, 887–896. [CrossRef]
19. Li, L.; Jiang, H.; Campbell, M.; Blanco, M.; Jane, J.-L. Characterization of maize amylose-extender (*ae*) mutant starches. Part I: Relationship between resistant starch contents and molecular structures. *Carbohydr. Polym.* **2008**, *74*, 396–404. [CrossRef]
20. Song, Y.; Jane, J. Characterization of barley starches of waxy, normal, and high amylose varieties. *Carbohydr. Polym.* **2000**, *41*, 365–377. [CrossRef]
21. Colonna, P.; Mercier, C. Macromolecular structure of wrinkled- and smooth-pea starch components. *Carbohydr. Res.* **1984**, *126*, 233–247. [CrossRef]
22. Wang, Y.-J.; White, P.; Pollak, L.; Jane, J. Amylopectin and intermediate materials in starches from mutant genotypes of the Oh43 inbred line. *Cereal Chem.* **1993**, *70*, 521–525.
23. Han, W.; Zhang, B.; Li, J.; Zhao, S.; Niu, M.; Jia, C.; Xiong, S. Understanding the fine structure of intermediate materials of maize starches. *Food Chem.* **2017**, *233*, 450–456. [CrossRef] [PubMed]
24. Waduge, R.N.; Kalinga, D.N.; Bertoft, E.; Seetharaman, K. Molecular structure and organization of starch granules from developing wheat endosperm. *Cereal Chem.* **2014**, *91*, 578–586. [CrossRef]
25. Han, X.-Z.; Benmoussa, M.; Gray, J.A.; BeMiller, J.N.; Hamaker, B.R. Detection of proteins in starch granule channels. *Cereal Chem.* **2005**, *82*, 351–355. [CrossRef]
26. Han, X.-Z.; Hamaker, B.R. Location of starch granule-associated proteins revealed by confocal laser scanning microscopy. *J. Cereal Sci.* **2002**, *35*, 109–116. [CrossRef]
27. Borén, M.; Glaring, M.A.; Ghebremedhin, H.; Olsson, H.; Blennow, A.; Jansson, C. Molecular and physicochemical characterization of the high-amylose barley mutant Amo1. *J. Cereal Sci.* **2008**, *47*, 79–89. [CrossRef]
28. Buléon, A.; Cotte, M.; Putaux, J.-L.; D'Hulst, C.; Susini, J. Tracking sulfur and phosphorus within single starch granules using synchrotron X-ray microfluorescence mapping. *Biochim. Biophys. Acta* **2014**, *1840*, 113–119. [CrossRef] [PubMed]

29. Kim, H.-S.; Huber, K.C. Channels within soft wheat starch A- and B-type granules. *J. Cereal Sci.* **2008**, *48*, 159–172. [CrossRef]
30. Hoover, R. Composition, molecular structure, and physicochemical properties of tuber and root starches: A review. *Carbohydr. Polym.* **2001**, *45*, 253–267. [CrossRef]
31. Waterschoot, J.; Gomand, S.V.; Fierens, E.; Delcour, J.A. Production, structure, physicochemical and functional properties of maize, cassava, wheat, potato and rice starches. *Starch/Stärke* **2015**, *67*, 14–29. [CrossRef]
32. Morrison, W.R. Starch lipids and how they relate to starch granule structure and functionality. *Cereal Foods World* **1995**, *40*, 437–446.
33. Morrison, W.R.; Milligan, T.P.; Azudin, M.N. A relationship between the amylose and lipid contents of starches from diploid cereals. *J. Cereal Sci.* **1984**, *2*, 257–271. [CrossRef]
34. Morrison, W.R.; Scott, D.C.; Karkalas, J. Variation in the composition and physical properties of barley starches. *Stärke* **1986**, *38*, 374–379. [CrossRef]
35. Shamekh, S.; Forssell, P.; Poutanen, K. Solubility pattern and recrystallization behavior of oat starch. *Starch/Stärke* **1994**, *46*, 129–133. [CrossRef]
36. Hizukuri, S.; Tabata, S.; Nikuni, Z. Studies on starch phosphate. Part 1. Estimation of glucose-6-phosphate residues in starch and the presence of other bound phosphate(s). *Starch/Stärke* **1970**, *22*, 338–343. [CrossRef]
37. Blennow, A.; Bay-Smidt, A.M.; Olsen, C.E.; Møller, B.L. The distribution of covalently bound phosphate in the starch granule in relation to starch crystallinity. *Int. J. Biol. Macromol.* **2000**, *27*, 211–218. [CrossRef]
38. Blennow, A.; Bay-Smidt, A.M.; Wischmann, B.; Olsen, C.E.; Lindberg-Møller, B. The degree of starch phosphorylation is related to the chain length distribution of the neutral and the phosphorylated chains of amylopectin. *Carbohydr. Res.* **1998**, *307*, 45–54. [CrossRef]
39. Blennow, A.; Engelsen, S.B.; Munck, L.; Møller, B.L. Starch molecular structure and phosphorylation investigated by a combined chromatographic and chemometric approach. *Carbohydr. Polym.* **2000**, *41*, 163–174. [CrossRef]
40. Blennow, A.; Engelsen, S.B. Helix-breaking news: Fighting crystalline starch energy deposits in the cell. *Trends Plant Sci.* **2010**, *15*, 236–240. [CrossRef] [PubMed]
41. Blennow, A.; Sjöland, A.K.; Andersson, R.; Kristiansson, P. The distribution of elements in the native starch granule as studied by particle-induced X-ray emission and complementary methods. *Anal. Biochem.* **2005**, *347*, 327–329. [CrossRef] [PubMed]
42. Ambigaipalan, P.; Hoover, R.; Donner, E.; Liu, Q.; Jaiswal, S.; Chibbar, R.; Nantanga, K.K.M.; Seetharaman, K. Structure of faba bean, black bean and pinto bean starches at different levels of granule organization and their physicochemical properties. *Food Res. Int.* **2011**, *44*, 2962–2974. [CrossRef]
43. Chen, P.; Yu, L.; Chen, L.; Li, X. Morphology and microstructure of maize starches with different amylose/amylopectin content. *Starch/Stärke* **2006**, *58*, 611–615. [CrossRef]
44. Varatharajan, V.; Hoover, R.; Li, J.; Vasanthan, T.; Nantanga, K.K.M.; Seetharaman, K.; Liu, Q.; Donner, E.; Jaiswal, S.; Chibbar, R.N. Impact of structural changes due to heat-moisture treatment at different temperatures on the susceptibility of normal and waxy potato starches towards hydrolysis by porcine pancreatic alpha amylase. *Food Res. Int.* **2011**, *44*, 2594–2606. [CrossRef]
45. French, D. Fine structure of starch and its relationship to the organization of starch granules. *J. Jpn. Soc. Starch Sci.* **1972**, *19*, 8–25. [CrossRef]
46. Robin, J.P.; Mercier, C.; Charbonnière, R.; Guilbot, A. Lintnerized starches. Gel filtration and enzymatic studies of insoluble residues from prolonged acid treatment of potato starch. *Cereal Chem.* **1974**, *51*, 389–406.
47. Biliaderis, C.G.; Grant, D.R.; Vose, J.R. Structural characterization of legume starches. II. Studies on acid-treated starches. *Cereal Chem.* **1981**, *58*, 502–507.
48. Wikman, J.; Blennow, A.; Buléon, A.; Putaux, J.-L.; Pérez, S.; Seetharaman, K.; Bertoft, E. Influence of amylopectin structure and degree of phosphorylation on the molecular composition of potato starch lintners. *Biopolymers* **2014**, *101*, 257–271. [CrossRef] [PubMed]
49. Srichuwong, S.; Isono, N.; Mishima, T.; Hisamatsu, M. Structure of linterized starch is related to X-ray diffraction pattern and susceptibility to acid and enzyme hydrolysis of starch granules. *Int. J. Biol. Macromol.* **2005**, *37*, 115–121. [CrossRef] [PubMed]
50. Wang, S.; Copeland, L. Effect of acid hydrolysis on starch structure and functionality: A review. *Crit. Rev. Food Sci. Nutr.* **2015**, *55*, 1081–1097. [CrossRef] [PubMed]

51. Bertoft, E. Lintnerisation of two amylose-free starches of A- and B-crystalline types, respectively. *Starch/Stärke* **2004**, *56*, 167–180. [CrossRef]
52. Wikman, J.; Blennow, A.; Bertoft, E. Effect of amylose deposition on potato tuber starch granule architecture and dynamics as studied by lintnerization. *Biopolymers* **2013**, *99*, 73–83. [CrossRef] [PubMed]
53. Imberty, A.; Pérez, S. Conformational analysis and molecular modelling of the branching point of amylopectin. *Int. J. Biol. Macromol.* **1989**, *11*, 177–185. [CrossRef]
54. Sanderson, J.S.; Daniels, R.D.; Donald, A.M.; Blennow, A.; Engelsen, S.B. Exploratory SAXS and HPAEC-PAD studies of starches from diverse plant genotypes. *Carbohydr. Polym.* **2006**, *64*, 433–443. [CrossRef]
55. Bogracheva, T.Y.; Morris, V.J.; Ring, S.G.; Hedley, C.L. The granular structure of C-type pea starch and its role in gelatinization. *Biopolymers* **1998**, *45*, 323–332. [CrossRef]
56. Buléon, A.; Gérard, C.; Riekel, C.; Vuong, R.; Chanzy, H. Details of the crystalline ultrastructure of C-starch granules revealed by synchrotron microfocus mapping. *Macromolecules* **1998**, *31*, 6605–6610. [CrossRef]
57. Popov, D.; Buléon, A.; Burghammer, M.; Chanzy, H.; Montesanti, N.; Putaux, J.-L.; Potocki-Véronèse, G.; Riekel, C. Crystal structure of A-amylose: A revisit from synchrotron microdiffraction analysis of single crystals. *Macromolecules* **2009**, *42*, 1167–1174. [CrossRef]
58. Imberty, A.; Pérez, S. A revisit to the three-dimensional structure of B-type starch. *Biopolymers* **1988**, *27*, 1205–1221. [CrossRef]
59. Buléon, A.; Colonna, P.; Planchot, V.; Ball, S. Starch granules: Structure and biosynthesis. *Int. J. Biol. Macromol.* **1998**, *23*, 85–112. [CrossRef]
60. Gomand, S.V.; Lamberts, L.; Derde, L.J.; Goesaert, H.; Vandeputte, G.E.; Goderis, B.; Visser, R.G.F.; Delcour, J.A. Structural properties and gelatinisation characteristics of potato and cassava starches and mutants thereof. *Food Hydrocoll.* **2010**, *24*, 307–317. [CrossRef]
61. Matalanis, A.M.; Campanella, O.H.; Hamaker, B.R. Storage retrogradation behavior of sorghum, maize and rice starch pastes related to amylopectin fine structure. *J. Cereal Sci.* **2009**, *50*, 74–81. [CrossRef]
62. Ren, S. Comparative analysis of some physicochemical properties of 19 kinds of native starches. *Starch/Stärke* **2017**, *68*, 1600367. [CrossRef]
63. Srichuwong, S.; Sunarti, T.C.; Mishima, T.; Isono, N.; Hisamatsu, M. Starches from different botanical sources I: Contribution of amylopectin fine structure to thermal properties and enzyme digestibility. *Carbohydr. Polym.* **2005**, *60*, 529–538. [CrossRef]
64. Sterling, C. A low angle spacing in starch. *J. Polym. Sci.* **1962**, *56*, S10–S12. [CrossRef]
65. Blazek, J.; Salman, H.; Rubio, A.L.; Gilbert, E.; Hanley, T.; Copeland, L. Structural characterization of wheat starch granules differing in amylose content and functional characteristics. *Carbohydr. Polym.* **2009**, *75*, 705–711. [CrossRef]
66. Jenkins, P.J.; Cameron, R.E.; Donald, A.M. A universal feature in the structure of starch granules from different botanical sources. *Starch/Stärke* **1993**, *45*, 417–420. [CrossRef]
67. Putaux, J.-L.; Molina-Boisseau, S.; Momaur, T.; Dufresne, A. Platelet nanocrystals resulting from the disruption of waxy maize starch granules by acid hydrolysis. *Biomacromolecules* **2003**, *4*, 1198–1202. [CrossRef] [PubMed]
68. Pérez, S.; Bertoft, E. The molecular structures of starch components and their contribution to the architecture of starch granules: A comprehensive review. *Starch/Stärke* **2010**, *62*, 389–420. [CrossRef]
69. Koroteeva, D.A.; Kiseleva, V.I.; Krivandin, A.V.; Shatalova, O.V.; Blaszczak, W.; Bertoft, E.; Piyachomkwan, K.; Yuryev, V.P. Structural and thermodynamic properties of rice starches with different genetic background. Part 2. Defectiveness of different supramolecular structures in starch granules. *Int. J. Biol. Macromol.* **2007**, *41*, 534–547. [CrossRef] [PubMed]
70. Kozlov, S.S.; Blennow, A.; Krivandin, A.V.; Yuryev, V.P. Structural and thermodynamic properties of starches extracted from GBSS and GWD suppressed potato lines. *Int. J. Biol. Macromol.* **2007**, *40*, 449–460. [CrossRef] [PubMed]
71. Kozlov, S.S.; Krivandin, A.V.; Shatalova, O.V.; Noda, T.; Bertoft, E.; Fornal, J.; Yuryev, V.P. Structure of starches extracted from near-isogenic wheat lines. Part II. Molecular organization of amylopectin clusters. *J. Therm. Anal. Calorim.* **2007**, *87*, 575–584. [CrossRef]
72. Jenkins, P.J.; Donald, A.M. The influence of amylose on starch granule structure. *Int. J. Biol. Macromol.* **1995**, *17*, 315–321. [CrossRef]

73. Donald, A.M.; Kato, K.L.; Perry, P.A.; Waigh, T.A. Scattering studies of the internal structure of starch granules. *Starch/Stärke* **2001**, *53*, 504–512. [CrossRef]
74. Gallant, D.J.; Bouchet, B.; Baldwin, P.M. Microscopy of starch: Evidence of a new level of granule organization. *Carbohydr. Polym.* **1997**, *32*, 177–191. [CrossRef]
75. Tang, H.; Mitsunaga, T.; Kawamura, Y. Molecular arrangement in blocklets and starch granules architecture. *Carbohydr. Polym.* **2006**, *63*, 555–560. [CrossRef]
76. Buttrose, M.S. The influence of environment on the shell structure of starch granules. *J. Cell Biol.* **1962**, *14*, 159–167. [CrossRef] [PubMed]
77. Pilling, E.; Smith, A.M. Growth ring formation in the starch granules of potato tubers. *Plant Physiol.* **2003**, *132*, 365–371. [CrossRef] [PubMed]
78. Sande-Bakhuizen, H.L.V.D. The structure of starch grains from wheat grown under constant conditions. *Proc. Soc. Exp. Biol. Med.* **1926**, *24*, 302–305. [CrossRef]
79. Goldstein, A.; Annor, G.; Vamadevan, V.; Tetlow, I.; Kirkensgaard, J.J.K.; Mortensen, K.; Blennow, A.; Hebelstrup, K.H.; Bertoft, E. Influence of diurnal photosynthetic activity on the morphology, structure, and thermal properties of normal and *waxy* barley starch. *Int. J. Biol. Macromol.* **2017**, *98*, 188–200. [CrossRef] [PubMed]
80. Huber, K.C.; BeMiller, J.N. Visualization of channels and cavities of corn and sorghum starch granules. *Cereal Chem.* **1997**, *74*, 537–541. [CrossRef]
81. Fannon, J.E.; Hauber, R.J.; BeMiller, J.N. Surface pores of starch granules. *Cereal Chem.* **1992**, *69*, 284–288.
82. Glaring, M.A.; Koch, C.B.; Blennow, A. Genotype-specific spatial distribution of starch molecules in the starch granule: A combined CLSM and SEM approach. *Biomacromolecules* **2006**, *7*, 2310–2320. [CrossRef] [PubMed]
83. Naguleswaran, S.; Li, J.; Vasanthan, T.; Bressler, D. Distribution of granule channels, protein, and phospholipid in triticale and corn starches as revealed by confocal laser scanning microscopy. *Cereal Chem.* **2011**, *88*, 87–94. [CrossRef]
84. Fannon, J.E.; Shull, J.M.; BeMiller, J.N. Interior channels of starch granules. *Cereal Chem.* **1993**, *70*, 611–613.
85. Huber, K.C.; BeMiller, J.N. Location of sites of reaction within starch granules. *Cereal Chem.* **2001**, *78*, 173–180. [CrossRef]
86. Gray, J.A.; BeMiller, J.N. Accessibility of starch granules to fatty acyl amides. *Cereal Chem.* **2001**, *78*, 236–242. [CrossRef]
87. Ohtani, T.; Yoshino, T.; Hagiwara, S.; Maekawa, T. High-resolution imaging of starch granule structure using atomic force microscopy. *Starch/Stärke* **2000**, *52*, 150–153. [CrossRef]
88. Baldwin, P.M.; Adler, J.; Davies, M.C.; Melia, C.D. High resolution imaging of starch granule surfaces by atomic force microscopy. *J. Cereal Sci.* **1998**, *27*, 255–265. [CrossRef]
89. Waduge, R.N.; Xu, S.; Bertoft, E.; Seetharaman, K. Exploring the surface morphology of developing wheat starch granules by using atomic force microscopy. *Starch/Stärke* **2013**, *65*, 398–409. [CrossRef]
90. Atkin, N.J.; Abeysekera, R.M.; Cheng, S.L.; Robards, A.W. An experimentally-based predictive model for the separation of amylopectin subunits during starch gelatinization. *Carbohydr. Polym.* **1998**, *36*, 173–192. [CrossRef]
91. Baker, A.A.; Miles, M.J.; Helbert, W. Internal structure of the starch granule revealed by AFM. *Carbohydr. Res.* **2001**, *330*, 249–256. [CrossRef]
92. Hanson, E.A.; Katz, J.R. Abhandlungen zur physikalischen Chemie der Stärke und der Brotbereitung. XVIII. Weitere Versuche die gewachsene Struktur des Stärkekorns mikroskopisch sichtbar zu machen. *Z. Physikal. Ch. (A)* **1934**, *169*, 135–142.
93. Hanson, E.A.; Katz, J.R. Abhandlungen zur physikalischen Chemie der Stärke und der Brotbereitung. XVII. Über Versuche die gewachsene Struktur des Stärkekorns mikroskopisch sichtbar zu machen besonders an lintnerisierter Stärke. *Z. Physikal. Ch. (A)* **1934**, *168*, 339–352.
94. Dang, J.M.C.; Copeland, L. Imaging rice grains using atomic force microscopy. *J. Cereal Sci.* **2003**, *37*, 165–170. [CrossRef]
95. Huang, J.; Wei, N.; Li, H.; Liu, S.; Yang, D. Outer shell, inner blocklets, and granule architecture of potato starch. *Carbohydr. Polym.* **2014**, *103*, 355–358. [CrossRef] [PubMed]
96. Chauhan, F.; Seetharaman, K. On the organization of chains in amylopectin. *Starch/Stärke* **2013**, *65*, 191–199. [CrossRef]

97. Buléon, A.; Bizot, H.; Delage, M.M.; Multon, J.L. Evolution of crystallinity and specific gravity of potato starch versus water ad- and desorption. *Starch/Stärke* **1982**, *34*, 361–366. [CrossRef]
98. Waigh, T.A.; Kato, K.L.; Donald, A.M.; Gidley, M.J.; Clarke, C.J.; Riekel, C. Side-chain liquid-crystalline model for starch. *Starch/Stärke* **2000**, *52*, 450–460. [CrossRef]
99. Perez-Herrera, M.; Vasanthan, T.; Hoover, R. Characterization of maize starch nanoparticles prepared by acid hydrolysis. *Cereal Chem.* **2017**, *93*, 323–330. [CrossRef]
100. Park, H.; Xu, S.; Seetharaman, K. A novel in situ atomic force microscopy imaging technique to probe surface morphological features of starch granules. *Carbohydr. Res.* **2011**, *346*, 847–853. [CrossRef] [PubMed]
101. Lineback, D.R. Current concepts of starch structure and its impact on properties. *J. Jpn. Soc. Starch Sci.* **1986**, *33*, 80–88. [CrossRef]
102. Zobel, H.F. Molecules to granules: A comprehensive starch review. *Starch/Stärke* **1988**, *40*, 44–50. [CrossRef]
103. Saibene, D.; Seetharaman, K. Amylose involvement in the amylopectin clusters from potato starch granules. *Carbohydr. Polym.* **2010**, *82*, 376–383. [CrossRef]
104. Schoch, T.J. Fractionation of starch by selective precipitation with butanol. *J. Am. Chem. Soc.* **1942**, *64*, 2957–2961. [CrossRef]
105. Takeda, Y.; Maruta, N.; Hizukuri, S. Structures of amylose subfractions with different molecular sizes. *Carbohydr. Res.* **1992**, *226*, 279–285. [CrossRef]
106. Takeda, Y.; Maruta, N.; Hizukuri, S. Examination of the structure of amylose by tritium labelling of the reducing terminal. *Carbohydr. Res.* **1992**, *227*, 113–120. [CrossRef]
107. Takeda, Y.; Shitaozono, T.; Hizukuri, S. Structures of sub-fractions of corn amylose. *Carbohydr. Res.* **1990**, *199*, 207–214. [CrossRef]
108. Takeda, Y.; Tomooka, S.; Hizukuri, S. Structures of branched and linear molecules of rice amylose. *Carbohydr. Res.* **1993**, *246*, 267–272. [CrossRef]
109. Takeda, Y.; Takeda, C.; Mizukami, H.; Hanashiro, I. Structures of large, medium and small starch granules of barley grain. *Carbohydr. Polym.* **1999**, *38*, 109–114. [CrossRef]
110. Takeda, Y.; Shitaozono, T.; Hizukuri, S. Molecular structure of corn starch. *Starch/Stärke* **1988**, *40*, 51–54. [CrossRef]
111. Shibanuma, K.; Takeda, Y.; Hizukuri, S.; Shibata, S. Molecular structures of some wheat starches. *Carbohydr. Polym.* **1994**, *25*, 111–116. [CrossRef]
112. Hanashiro, I.; Takeda, Y. Examination of number-average degree of polymerization and molar-based distribution of amylose by fluorescent labeling with 2-aminopyridine. *Carbohydr. Res.* **1998**, *306*, 421–426. [CrossRef]
113. Takeda, Y.; Hizukuri, S.; Juliano, B.O. Structures and amounts of branched molecules in rice amyloses. *Carbohydr. Res.* **1989**, *186*, 163–166. [CrossRef]
114. Morrison, W.R.; Laignelet, B. An improved colorimetric procedure for determining apparent and total amylose in cereal and other starches. *J. Cereal Sci.* **1983**, *1*, 9–20. [CrossRef]
115. Fredriksson, H.; Silverio, J.; Andersson, R.; Eliasson, A.-C.; Åman, P. The influence of amylose and amylopectin characteristics on gelatinization and retrogradation properties of different starches. *Carbohydr. Polym.* **1998**, *35*, 119–134. [CrossRef]
116. Wang, L.Z.; White, P.J. Structure and physicochemical properties of starches from oats with different lipid contents. *Cereal Chem.* **1994**, *71*, 443–450.
117. Manelius, R.; Bertoft, E. The effect of Ca^{2+}-ions on the α-amylolysis of granular starches from oats and waxy-maize. *J. Cereal Sci.* **1996**, *24*, 139–150. [CrossRef]
118. Ao, Z.; Jane, J.-L. Characterization and modeling of the A- and B-granule starches of wheat, triticale, and barley. *Carbohydr. Polym.* **2007**, *67*, 46–55. [CrossRef]
119. Blennow, A.; Bay-Smidt, A.M.; Bauer, R. Amylopectin aggregation as a function of starch phosphate content studied by size exclusion chromatography and on-line refractive index and light scattering. *Int. J. Biol. Macromol.* **2001**, *28*, 409–420. [CrossRef]
120. Franco, C.M.L.; Wong, K.-S.; Yoo, S.-H.; Jane, J.-L. Structural and functional characteristics of selected soft wheat starches. *Cereal Chem.* **2002**, *79*, 243–248. [CrossRef]
121. Gidley, M.J.; Cooke, D.; Darke, A.H.; Hoffmann, R.A.; Russell, A.L.; Greenwell, P. Molecular order and structure in enzyme-resistant retrograded starch. *Carbohydr. Polym.* **1995**, *28*, 23–31. [CrossRef]

122. Grant, L.A.; Ostenson, A.M.; Rayas-Duarte, P. Determination of amylose and amylopectin of wheat starch using high performance size-exclusion chromatography (HPSEC). *Cereal Chem.* **2002**, *79*, 771–773. [CrossRef]
123. Jane, J.; Chen, Y.Y.; Lee, L.F.; McPherson, A.E.; Wong, K.S.; Radosavljevic, M.; Kasemsuwan, T. Effects of amylopectin branch chain length and amylose content on gelatinization and pasting properties of starch. *Cereal Chem.* **1999**, *76*, 629–637. [CrossRef]
124. Rollings, J. Enzymatic depolymerization of polysaccharides. *Carbohydr. Polym.* **1985**, *5*, 37–82. [CrossRef]
125. Sasaki, T.; Matsuki, J. Effect of wheat starch structure on swelling power. *Cereal Chem.* **1998**, *75*, 525–529. [CrossRef]
126. Takeda, Y.; Hizukuri, S.; Juliano, B.O. Purification and structure of amylose from rice starch. *Carbohydr. Res.* **1986**, *148*, 299–308. [CrossRef]
127. Takeda, Y.; Preiss, J. Structures of B90 (*sugary*) and W64A (normal) maize starches. *Carbohydr. Res.* **1993**, *240*, 265–275. [CrossRef]
128. Verwimp, T.; Vandeputte, G.E.; Marrant, K.; Delcour, J.A. Isolation and characterisation of rye starch. *J. Cereal Sci.* **2004**, *39*, 85–90. [CrossRef]
129. Yoshimoto, Y.; Takenoushi, T.; Takeda, Y. Molecular structure and some physicochemical properties of waxy and low-amylose barley starches. *Carbohydr. Polym.* **2002**, *47*, 159–167. [CrossRef]
130. Takeda, Y.; Shirasaka, K.; Hizukuri, S. Examination of the purity and structure of amylose by gel-permeation chromatography. *Carbohydr. Res.* **1984**, *132*, 83–92. [CrossRef]
131. Yusuph, M.; Tester, R.F.; Ansell, R.; Snape, C.E. Composition and properties of starches extracted from tubers of different potato varieties grown under the same environmental conditions. *Food Chem.* **2003**, *82*, 283–289. [CrossRef]
132. Hanashiro, I.; Sakaguchi, I.; Yamashita, H. Branched structures of rice amylose examined by differential fluorescence detection of side-chain distribution. *J. Appl. Glycosci.* **2013**, *60*, 79–85. [CrossRef]
133. Jane, J.-L. Mechanism of starch gelatinization in neutral salt solutions. *Starch/Stärke* **1993**, *45*, 161–166. [CrossRef]
134. Koch, K.; Jane, J.-L. Morphological changes of granules of different starches by surface gelatinization with calcium chloride. *Cereal Chem.* **2000**, *77*, 115–120. [CrossRef]
135. Kuakpetoon, D.; Wang, Y.-J. Internal structure and physicochemical properties of corn starches as revealed by chemical surface gelatinization. *Carbohydr. Res.* **2007**, *342*, 2253–2263. [CrossRef] [PubMed]
136. Jane, J.-L.; Shen, J.J. Internal structure of the potato starch granule revealed by chemical gelatinization. *Carbohydr. Res.* **1993**, *247*, 279–290. [CrossRef]
137. Pan, D.D.; Jane, J.-L. Internal structure of normal maize starch granules revealed by chemical surface gelatinization. *Biomacromolecules* **2000**, *1*, 126–132. [CrossRef] [PubMed]
138. Blennow, A.; Hansen, M.; Schulz, A.; Jørgensen, K.; Donald, A.M.; Sanderson, J. The molecular deposition of transgenically modified starch in the starch granule as imaged by functional microscopy. *J. Struct. Biol.* **2003**, *143*, 229–241. [CrossRef] [PubMed]
139. Myllärinen, P.; Autio, K.; Schulman, A.H.; Poutanen, K. Heat-induced changes of small and large barley starch granules. *J. Inst. Brew.* **1998**, *104*, 343–349. [CrossRef]
140. Patel, B.K.; Saibene, D.; Seetharaman, K. Restriction of starch granule swelling by iodine during heating. *Cereal Chem.* **2006**, *83*, 173–178. [CrossRef]
141. Jane, J.-L.; Xu, A.; Radosavljevic, M.; Seib, P.A. Location of amylose in normal starch granules. I. Susceptibility of amylose and amylopectin to cross-linking reagents. *Cereal Chem.* **1992**, *69*, 405–409.
142. Kozlov, S.S.; Noda, T.; Bertoft, E.; Yuryev, V.P. Structure of starches extracted from near isogenic wheat lines. Part I. Effect of different GBSS I combinations. *J. Therm. Anal. Calorim.* **2006**, *86*, 291–301. [CrossRef]
143. Kiseleva, V.I.; Krivandin, A.V.; Fornal, J.; Blaszczak, W.; Jelinski, T.; Yuryev, V.P. Annealing of normal and mutant wheat starches. LM, SEM, DSC, and SAXS studies. *Carbohydr. Res.* **2005**, *340*, 75–83. [CrossRef] [PubMed]
144. Koroteeva, D.A.; Kiseleva, V.I.; Sriroth, K.; Piyachomkwan, K.; Bertoft, E.; Yuryev, P.V.; Yuryev, V.P. Structural and thermodynamic properties of rice starches with different genetic background. Part 1. Differentiation of amylopectin and amylose defects. *Int. J. Biol. Macromol.* **2007**, *41*, 391–403. [CrossRef] [PubMed]
145. Banks, W.; Greenwood, C.T. *Starch and Its Components*; Edinburgh University Press: Edinburgh, UK, 1975.
146. Banks, W.; Greenwood, C.T. The conformation of amylose in dilute solution. *Starch/Stärke* **1971**, *23*, 300–314. [CrossRef]

147. Cheetham, N.W.H.; Tao, L. Amylose conformational transitions in binary DMSO/water mixtures. *Starch/Stärke* **1997**, *49*, 407–415. [CrossRef]
148. Hamori, E.; Senior, M.B. Kinetic and hydrodynamic studies relating to the structure of the amylose macromolecule in aqueous solution. *Ann. N. Y. Acad. Sci.* **1973**, *210*, 34–38. [CrossRef] [PubMed]
149. Elmgren, H. Helical conformation of amylose in aqueous solution. I. Viscosity measurements. *Biopolymers* **1984**, *23*, 2525–2541. [CrossRef]
150. Kodama, M.; Noda, H.; Katama, T. Conformation of amylose in water. I. Light-scattering and sedimentation-equilibrium measurements. *Biopolymers* **1978**, *17*, 985–1002. [CrossRef]
151. Senior, M.B.; Hamori, E. Investigation of the effect of amylose/iodine complexation on the conformation of amylose in aqueous solution. *Biopolymers* **1973**, *12*, 65–78. [CrossRef]
152. Hayashi, A.; Kinoshita, K.; Miyake, Y. The conformation of amylose in solution. I. *Polymer J.* **1981**, *13*, 537–541. [CrossRef]
153. Pfannemüller, B.; Mayerhöfer, H.; Schulz, R.C. Conformation of amylose in aqueous solution: Optical rotatory dispersion and circular dichroism of amylose-iodine complexes and dependence on chain lenght of retrogradation of amylose. *Biopolymers* **1971**, *10*, 243–261. [CrossRef]
154. Gidley, M.J. Molecular mechanisms underlying amylose aggregation and gelation. *Macromolecules* **1989**, *22*, 351–358. [CrossRef]
155. French, A.D. Allowed and preferred shapes of amylose. *Bakers Digest* **1979**, *53*, 39–54.
156. French, A.D.; Murphy, V.G. Computer modeling in the study of starch. *Cereal Foods World* **1977**, *22*, 61–70.
157. Katz, J.R.; Itallie, T.B.V. Abhandlungen zur physikalischen Chemie der Stärke und der Brotbereitung. V. Alle Stärkearten haben das gleiche Retrogradtionsspektrum. *Z. Physikal. Ch. (A)* **1930**, *150*, 90–99.
158. Gernat, C.; Radosta, S.; Anger, H.; Damaschun, G. Crystalline parts of three different conformations detected in native and enzymatically degraded starches. *Starch/Stärke* **1993**, *45*, 309–314. [CrossRef]
159. Waduge, R.N.; Xu, S.; Seetharaman, K. Iodine absorption properties and its effect on the crystallinity of developing wheat starch granules. *Carbohydr. Polym.* **2010**, *82*, 786–794. [CrossRef]
160. Vamadevan, V.; Hoover, R.; Bertoft, E.; Seetharaman, K. Hydrothermal treatment and iodine binding provide insights into the organization of glucan chains within the semi-crystalline lamellae of corn starch granules. *Biopolymers* **2014**, *101*, 871–885. [CrossRef] [PubMed]
161. Varatharajan, V.; Hoover, R.; Liu, Q.; Seetharaman, K. The impact of heat-moisture treatment on the molecular structure and physicochemical properties of normal and waxy potato starches. *Carbohydr. Polym.* **2010**, *81*, 466–475. [CrossRef]
162. Morrison, W.R.; Law, R.V.; Snape, C.E. Evidence for inclusion complexes of lipids with V-amylose in maize, rice and oat starches. *J. Cereal Sci.* **1993**, *18*, 107–109. [CrossRef]
163. Aberle, T.; Burchard, W.; Vorwerg, W.; Radosta, S. Conformational contributions of amylose and amylopectin to the structural properties of starches from various sources. *Starch/Stärke* **1994**, *46*, 329–335. [CrossRef]
164. Banks, W.; Greenwood, C.T.; Walker, J.T. Studies on the starches of barley genotypes: The waxy starch. *Starch/Stärke* **1970**, *22*, 149–152. [CrossRef]
165. Lelievre, J.; Lewis, J.A.; Marsden, K. The size and shape of amylopectin: A study using analytical ultracentrifugation. *Carbohydr. Res.* **1986**, *153*, 195–203. [CrossRef]
166. Perez-Rea, D.; Bergenståhl, B.; Nilsson, L. Development and evaluation of methods for starch dissolution using asymmetrical flow field-flow fractionation. Part I: Dissolution of amylopectin. *Anal. Bioanal. Chem.* **2015**, *407*, 4315–4326. [CrossRef] [PubMed]
167. Yokoyama, W.; Renner-Nantz, J.J.; Shoemaker, C.F. Starch molecular mass and size by size-exclusion chromatography in DMSO-LiBr coupled with multiple angle laser light scattering. *Cereal Chem.* **1998**, *75*, 530–535. [CrossRef]
168. McIntyre, A.P.; Mukerjea, R.; Robyt, J.F. Reducing values: Dinitrosalicylate gives over-oxidation and invalid results whereas copper bicinchoninate gives no over-oxidation and valid results. *Carbohydr. Res.* **2013**, *380*, 118–123. [CrossRef] [PubMed]
169. Charoenkul, N.; Uttapap, D.; Pathipanawat, W.; Takeda, Y. Molecular structure of starches from cassava varieties having different cooked root textures. *Starch/Stärke* **2006**, *58*, 443–452. [CrossRef]
170. Stacy, C.J.; Foster, J.F. Molecular weight heterogeneity in starch amylopectins. *J. Polym. Sci. Part A* **1957**, *25*, 39–50. [CrossRef]

171. Takeda, Y.; Shibahara, S.; Hanashiro, I. Examination of the structure of amylopectin molecules by fluorescent labeling. *Carbohydr. Res.* **2003**, *338*, 471–475. [CrossRef]
172. Hizukuri, S. Relationship between the distribution of the chain length of amylopectin and the crystalline structure of starch granules. *Carbohydr. Res.* **1985**, *141*, 295–306. [CrossRef]
173. Kalichevsky, M.T.; Orford, P.D.; Ring, S.G. The retrogradation and gelation of amylopectins from various botanical sources. *Carbohydr. Res.* **1990**, *198*, 49–55. [CrossRef]
174. Boyer, C.D.; Liu, K.-C. The interaction of endosperm genotype and genetic background. Part I. Differences in chromatographic profiles of starches from nonmutant and mutant endosperms. *Starch/Stärke* **1985**, *37*, 73–79. [CrossRef]
175. Koizumi, K.; Fukuda, M.; Hizukuri, S. Estimation of the distributions of chain length of amylopectins by high-performance liquid chromatography with pulsed amperometric detection. *J. Chromatogr.* **1991**, *585*, 233–238. [CrossRef]
176. Morell, M.K.; Samuel, M.S.; O'Shea, M.G. Analysis of starch structure using fluorophore-assisted carbohydrate electrophoresis. *Electrophoresis* **1998**, *19*, 2603–2611. [CrossRef] [PubMed]
177. O'Shea, M.G.; Morell, M.K. High resolution slab gel electrophoresis of 8-amino-1,3,6-pyrenetrisulfonic acid (APTS) tagged oligosaccharides using a DNA sequencer. *Electrophoresis* **1996**, *17*, 681–686. [CrossRef] [PubMed]
178. O'Shea, M.G.; Samuel, M.S.; Konik, C.M.; Morell, M.K. Fluorophore-assisted carbohydrate electrophoresis (FACE) of oligosaccharides: Efficiency of labelling and high-resolution separation. *Carbohydr. Res.* **1998**, *307*, 1–12. [CrossRef]
179. Peat, S.; Whelan, W.J.; Thomas, G.J. Evidence of multiple branching in waxy maize starch. *J. Chem. Soc.* **1952**, 4546–4548.
180. Hizukuri, S. Polymodal distribution of the chain lengths of amylopectins, and its significance. *Carbohydr. Res.* **1986**, *147*, 342–347. [CrossRef]
181. Hanashiro, I.; Itoh, K.; Kuratomi, Y.; Yamazaki, M.; Igarashi, T.; Matsugasako, J.-I.; Takeda, Y. Granule-bound starch synthase I is responsible for biosynthesis of extra-long unit chains of amylopectin in rice. *Plant Cell Physiol.* **2008**, *49*, 925–933. [CrossRef] [PubMed]
182. Takeda, Y.; Hizukuri, S.; Juliano, B.O. Structures of rice amylopectins with low and high affinities for iodine. *Carbohydr. Res.* **1987**, *168*, 79–88. [CrossRef]
183. Charoenkul, N.; Uttapap, D.; Pathipanawat, W.; Takeda, Y. Simultaneous determination of amylose content & unit chain distribution of amylopectins of cassava starches by fluorescent labeling/HPSEC. *Carbohydr. Polym.* **2006**, *65*, 102–108.
184. Yoo, S.-H.; Jane, J.-L. Structural and physical characteristics of waxy and other wheat starches. *Carbohydr. Polym.* **2002**, *49*, 297–305. [CrossRef]
185. Noda, T.; Takigawa, S.; Matsuura-Endo, C.; Kim, S.-J.; Hashimoto, N.; Yamauchi, H.; Hanashiro, I.; Takeda, Y. Physicochemical properties and amylopectin structures of large, small, and extremely small potato starch granules. *Carbohydr. Polym.* **2005**, *60*, 245–251. [CrossRef]
186. Hanashiro, I.; Matsugasako, J.-I.; Egashira, T.; Takeda, Y. Structural characterization of long unit-chains of amylopectin. *J. Appl. Glycosci.* **2005**, *52*, 233–237. [CrossRef]
187. Laohaphatanaleart, K.; Piyachomkwan, K.; Sriroth, K.; Santisopasri, V.; Bertoft, E. A study of the internal structure in cassava and rice amylopectin. *Starch/Stärke* **2009**, *61*, 557–569. [CrossRef]
188. Hanashiro, I.; Tagawa, M.; Shibahara, S.; Iwata, K.; Takeda, Y. Examination of molar-based distribution of A, B and C chains of amylopectin by fluorescent labeling with 2-aminopyridine. *Carbohydr. Res.* **2002**, *337*, 1211–1215. [CrossRef]
189. Annor, G.A.; Marcone, M.; Bertoft, E.; Seetharaman, K. Unit and internal chain profile of millet amylopectin. *Cereal Chem.* **2014**, *91*, 29–34. [CrossRef]
190. Gayin, J.; Abdel-Aal, E.-S.M.; Manful, J.; Bertoft, E. Unit and internal chain profile of African rice (*Oryza glaberrima*) amylopectin. *Carbohydr. Polym.* **2016**, *137*, 466–472. [CrossRef] [PubMed]
191. Goldstein, A.; Annor, G.; Blennow, A.; Bertoft, E. Effect of diurnal photosynthetic activity on the fine structure of amylopectin from normal and waxy barley starch. *Int. J. Biol. Macromol.* **2017**, *102*, 924–932. [CrossRef] [PubMed]

192. Kalinga, D.N.; Waduge, R.; Liu, Q.; Yada, R.Y.; Bertoft, E.; Seetharaman, K. On the differences in granular architechture and starch structure between pericarp and endosperm wheat starches. *Starch/Stärke* **2013**, *65*, 791–800. [CrossRef]
193. Kong, X.; Bertoft, E.; Bao, J.; Corke, H. Molecular structure of amylopectin from amaranth starch and its effect on physicochemical properties. *Int. J. Biol. Macromol.* **2008**, *43*, 377–382. [CrossRef] [PubMed]
194. Zhu, F.; Bertoft, E.; Källman, A.; Myers, A.M.; Seetharaman, K. Molecular structure of starches from maize mutants deficient in starch synthase III. *J. Agric. Food Chem.* **2013**, *61*, 9899–9907. [CrossRef] [PubMed]
195. Manners, D.J. Recent developments in our understanding of amylopectin structure. *Carbohydr. Polym.* **1989**, *11*, 87–112. [CrossRef]
196. Bertoft, E. Investigation of the fine structure of alpha-dextrins derived from amylopectin and their relation to the structure of waxy-maize starch. *Carbohydr. Res.* **1991**, *212*, 229–244. [CrossRef]
197. Matheson, N.K. The chemical structure of amylose and amylopectin fractions of starch from tobacco leaves during development and diurnally-nocturnally. *Carbohydr. Res.* **1996**, *282*, 247–262. [CrossRef]
198. Hanes, C.S. The reversible formation of starch from glucose-1-phosphate catalysed by potato phosphorylase. *Proc. R. Soc. Lond. B* **1940**, *129*, 174–208. [CrossRef]
199. Hestrin, S. Action pattern of crystalline muscle phosphorylase. *J. Biol. Chem.* **1949**, *179*, 943–955. [PubMed]
200. Meyer, K.H. The past and present of starch chemistry. *Experientia* **1952**, *8*, 405–444. [CrossRef] [PubMed]
201. Walker, G.J.; Whelan, W.J. The mechanism of carbohydrase action. 8. Structures of the muscle-phosphorylase limit dextrins of glycogen and amylopectin. *Biochem. J.* **1960**, *76*, 264–268. [CrossRef] [PubMed]
202. Bertoft, E. Partial characterisation of amylopectin alpha-dextrins. *Carbohydr. Res.* **1989**, *189*, 181–193. [CrossRef]
203. Bertoft, E. On the nature of categories of chains in amylopectin and their connection to the super helix model. *Carbohydr. Polym.* **2004**, *57*, 211–224. [CrossRef]
204. Summer, R.; French, D. Action of β-amylase on branched oligosaccharides. *J. Biol. Chem.* **1956**, *222*, 469–477.
205. Akai, H.; Yokobayashi, K.; Misaki, A.; Harada, T. Complete hydrolysis of branching linkages in glycogen by Pseudomonas isoamylase: Distribution of linear chains. *Biochim. Biophys. Acta* **1971**, *237*, 422–429. [CrossRef]
206. Harada, T.; Misaki, A.; Akai, H.; Yokobayashi, K.; Sugimoto, K. Characterization of *Pseudomonas* isoamylase by its actions on amylopectin and glycogen: Comparison with *Aerobacter* pullulanase. *Biochim. Biophys. Acta* **1972**, *268*, 497–505. [CrossRef]
207. Yokobayashi, K.; Akai, H.; Sugimoto, T.; Hirao, M.; Sugimoto, K.; Harada, T. Comparison of the kinetic parameters of *Pseudomonas* isoamylase and *Aerobacter* pullulanase. *Biochim. Biophys. Acta* **1973**, *293*, 197–202. [CrossRef]
208. Yokobayashi, K.; Misaki, A.; Harada, T. Purification and properties of Pseudomonas isoamylase. *Biochim. Biophys. Acta* **1970**, *212*, 458–469. [CrossRef]
209. Kainuma, K.; Kobayashi, S.; Harada, T. Action of *Pseudomonas* isoamylase on various branched oligo- and polysaccharides. *Carbohydr. Res.* **1978**, *61*, 345–357. [CrossRef]
210. Gidley, M.J.; Bulpin, P.V. Crystallisation of malto-oligosaccharides as models of the crystalline forms of starch: Minimum chain-length requirement for the formation of double helices. *Carbohydr. Res.* **1987**, *161*, 291–300. [CrossRef]
211. Kong, X.; Corke, H.; Bertoft, E. Fine structure characterization of amylopectins from grain amaranth starch. *Carbohydr. Res.* **2009**, *344*, 1701–1708. [CrossRef] [PubMed]
212. Kalinga, D.N.; Bertoft, E.; Tetlow, I.; Liu, Q.; Yada, R.Y.; Seetharaman, K. Evolution of amylopectin structure in developing wheat endosperm. *Carbohydr. Polym.* **2014**, *112*, 316–324. [CrossRef] [PubMed]
213. Bijttebier, A.; Goesaert, H.; Delcour, J.A. Hydrolysis of amylopectin by amylolytic enzymes: Structural analysis of the residual amylopectin population. *Carbohydr. Res.* **2010**, *345*, 235–242. [CrossRef] [PubMed]
214. Robyt, J.; French, D. Action pattern and specificity of an amylase from *Bacillus subtilis*. *Arch. Biochem. Biophys.* **1963**, *100*, 451–467. [CrossRef]
215. Thoma, J.A.; Brothers, C.; Spradlin, J. Subsite mapping of enzymes. Studies on *Bacillus subtilis* amylase. *Biochemistry* **1970**, *9*, 1768–1775. [CrossRef] [PubMed]
216. Bertoft, E. Hydrolysis of amylopectin by the alpha-amylase of *B. subtilis*. *Carbohydr. Res.* **1986**, *149*, 379–387. [CrossRef]
217. Bertoft, E. The Use of Alpha-Amylase in Structural Studies of Amylopectin. Ph.D. Thesis, Åbo Akademi University, Turku, Finland, 1990.

218. Bertoft, E.; Koch, K. Composition of chains in waxy-rice starch and its structural units. *Carbohydr. Polym.* **2000**, *41*, 121–132. [CrossRef]
219. Bertoft, E.; Qin, Z.; Manelius, R. Studies on the structure of pea starches. Part 3: Amylopectin of smooth pea starch. *Starch/Stärke* **1993**, *45*, 377–382. [CrossRef]
220. Bertoft, E.; Åvall, A.-K. Structural analysis on the amylopectin of waxy-barley large starch granules. *J. Inst. Brew.* **1992**, *98*, 433–437. [CrossRef]
221. Gérard, C.; Planchot, V.; Colonna, P.; Bertoft, E. Relationship between branching density and crystalline structure of A- and B-type maize mutant starches. *Carbohydr. Res.* **2000**, *326*, 130–144. [CrossRef]
222. Zhu, Q.; Bertoft, E. Composition and structural analysis of alpha-dextrins from potato amylopectin. *Carbohydr. Res.* **1996**, *288*, 155–174. [CrossRef]
223. Bertoft, E. Composition of building blocks in clusters from potato amylopectin. *Carbohydr. Polym.* **2007**, *70*, 123–136. [CrossRef]
224. Bertoft, E.; Zhu, Q.; Andtfolk, H.; Jungner, M. Structural heterogeneity in waxy-rice starch. *Carbohydr. Polym.* **1999**, *38*, 349–359. [CrossRef]
225. Laohaphatanaleart, K.; Piyachomkwan, K.; Sriroth, K.; Bertoft, E. The fine structure of cassava amylopectin. Part 1. Organization of clusters. *Int. J. Biol. Macromol.* **2010**, *47*, 317–324. [CrossRef] [PubMed]
226. Zhu, F.; Corke, H.; Åman, P.; Bertoft, E. Structures of clusters in sweetpotato amylopectin. *Carbohydr. Res.* **2011**, *346*, 1112–1121. [CrossRef] [PubMed]
227. Bertoft, E. Composition of clusters and their arrangement in potato amylopectin. *Carbohydr. Polym.* **2007**, *68*, 433–446. [CrossRef]
228. Bertoft, E.; Källman, A.; Koch, K.; Andersson, R.; Åman, P. The cluster structure of barley amylopectins of different genetic backgrounds. *Int. J. Biol. Macromol.* **2011**, *49*, 441–453. [CrossRef] [PubMed]
229. Bertoft, E.; Koch, K.; Åman, P. Building block organisation of clusters in amylopectin of different structural types. *Int. J. Biol. Macromol.* **2012**, *50*, 1212–1223. [CrossRef] [PubMed]
230. Zhu, F.; Corke, H.; Åman, P.; Bertoft, E. Structures of building blocks in clusters of sweetpotato amylopectin. *Carbohydr. Res.* **2011**, *346*, 2913–2925. [CrossRef] [PubMed]
231. Bertoft, E.; Källman, A.; Koch, K.; Andersson, R.; Åman, P. The building block structure of barley amylopectin. *Int. J. Biol. Macromol.* **2011**, *49*, 900–909. [CrossRef] [PubMed]
232. Bertoft, E.; Laohaphatanaleart, K.; Piyachomkwan, K.; Sriroth, K. The fine structure of cassava amylopectin. Part 2. Building block structure of clusters. *Int. J. Biol. Macromol.* **2010**, *47*, 325–335. [CrossRef] [PubMed]
233. Bertoft, E.; Koch, K.; Åman, P. Structure of building blocks in amylopectins. *Carbohydr. Res.* **2012**, *361*, 105–113. [CrossRef] [PubMed]
234. Gayin, J.; Abdel-Aal, E.-S.M.; Marcone, M.; Manful, J.; Bertoft, E. Structure of clusters and building blocks in amylopectin from African rice accessions. *Carbohydr. Polym.* **2016**, *148*, 125–133. [CrossRef] [PubMed]
235. Kalinga, D.N.; Bertoft, E.; Tetlow, I.; Seetharaman, K. Structure of clusters and building blocks in amylopectin from developing wheat endosperm. *Carbohydr. Polym.* **2014**, *112*, 325–333. [CrossRef] [PubMed]
236. Zhu, F.; Bertoft, E.; Seetharaman, K. Composition of clusters and building blocks in amylopectins of starch mutants deficient in starch synthase III. *J. Agric. Food Chem.* **2013**, *61*, 12345–12355. [CrossRef] [PubMed]
237. Zhu, F.; Bertoft, E.; Szydlowski, N.; D'Hulst, C.; Seetharaman, K. Branching patterns in leaf starches from *Arabidopsis* mutants deficient in diverse starch synthases. *Carbohydr. Res.* **2015**, *401*, 96–108. [CrossRef] [PubMed]
238. Kalinga, D.N.; Bertoft, E. Internal structure of amylopectin from the pericarp tissue of developing wheat kernels. *Starch/Stärke* **2015**, *67*, 1070–1076. [CrossRef]
239. Peymanpour, G.; Marcone, M.; Ragaee, S.; Tetlow, I.; Lane, C.C.; Seetharaman, K.; Bertoft, E. On the molecular structure of the amylopectin fraction isolated from "high-amylose" *ae* maize starches. *Int. J. Biol. Macromol.* **2016**, *91*, 768–777. [CrossRef] [PubMed]
240. Vamadevan, V.; Bertoft, E.; Seetharaman, K. On the importance of organization of glucan chains on thermal properties of starch. *Carbohydr. Polym.* **2013**, *92*, 1653–1659. [CrossRef] [PubMed]
241. Seetharaman, K.; Bertoft, E. Perspectives on the history of research on starch. Part V: On the conceptualization of amylopectin structure. *Starch/Stärke* **2013**, *65*, 1–7. [CrossRef]
242. Nikuni, Z. Starch and cooking. *Sci. Cook.* **1969**, *2*, 6–14. (In Japanese)

243. Jacobs, H.; Eerlingen, R.C.; Rouseu, N.; Colonna, P.; Delcour, J.A. Acid hydrolysis of native and annealed wheat, potato and pea starches—DSC melting features and chain length distributions of lintnerised starches. *Carbohydr. Res.* **1998**, *308*, 359–371. [CrossRef]
244. Akai, H.; Yokobayashi, K.; Misaki, A.; Harada, T. Structural analysis of amylopectin using *Pseudomonas isoamylase*. *Biochim. Biophys. Acta* **1971**, *252*, 427–431. [CrossRef]
245. Manners, D.J.; Matheson, N.K. The fine structure of amylopectin. *Carbohydr. Res.* **1981**, *90*, 99–110. [CrossRef]
246. Bender, H.; Siebert, R.; Stadler-Szöke, A. Can cyclodextrin glycosyltransferase be useful for the investigation of the fine structure of amylopectins? Characterisation of highly branched clusters isolated from digests with potato and maize starches. *Carbohydr. Res.* **1982**, *110*, 245–259. [CrossRef]
247. Finch, P.; Sebesta, D.W. The amylase of *Pseudomonas stutzeri* as a probe of the structure of amylopectin. *Carbohydr. Res.* **1992**, *227*, c1–c4. [CrossRef]
248. Bertoft, E.; Henriksnäs, H. Initial stages in α-amylolysis of barley starch. *J. Inst. Brew.* **1982**, *88*, 261–265. [CrossRef]
249. O'Sullivan, A.C.; Pérez, S. The relationship between internal chain length of amylopectin and crystallinity in starch. *Biopolymers* **1999**, *50*, 381–390. [CrossRef]
250. Bertoft, E. On the building block and backbone concepts of amylopectin structure. *Cereal Chem.* **2013**, *90*, 294–311. [CrossRef]
251. Källman, A.; Bertoft, E.; Koch, K.; Åman, P.; Andersson, R. On the interconnection of clusters and building blocks in barley amylopectin. *Int. J. Biol. Macromol.* **2013**, *55*, 75–82. [CrossRef] [PubMed]
252. Bertoft, E.; Nilsson, L. Starch. Analytical and structural aspects. In *Carbohydrates in Food*; Eliasson, A.-C., Ed.; CRC Press, Taylor & Francis Group: Boca Raton, FL, USA, 2017; pp. 377–478.
253. Ball, S.; Guan, H.-P.; James, M.; Myers, A.; Keeling, P.; Mouille, G.; Buléon, A.; Colonna, P.; Preiss, J. From glycogen to amylopectin: A model for the biogenesis of the plant starch granule. *Cell* **1996**, *86*, 349–352. [CrossRef]
254. Debet, M.R.; Gidley, M.J. Three classes of starch granule swelling: Influence of surface proteins and lipids. *Carbohydr. Polym.* **2006**, *64*, 452–465. [CrossRef]
255. Qi, X.; Tester, R.F.; Snape, C.E.; Ansell, R. Molecular basis of the gelatinisation and swelling characteristics of waxy rice starches grown in the same location during the same season. *J. Cereal Sci.* **2003**, *37*, 363–376. [CrossRef]
256. Tester, R.F.; Morrison, W.R. Swelling and gelatinization of cereal starches. I. Effects of amylopectin, amylose, and lipids. *Cereal Chem.* **1990**, *67*, 551–557.
257. Dhillon, S.; Abdel-Aal, E.-S.M.; Seetharaman, K. Effect of iodine on polymer leaching and granule swelling of starches from different sources. *J. Cereal Sci.* **2011**, *54*, 76–82. [CrossRef]
258. Jenkins, P.J.; Donald, A.M. Gelatinisation of starch: A combined SAXS/WAXS/DSC and SANS study. *Carbohydr. Res.* **1998**, *308*, 133–147. [CrossRef]
259. Singh, N.; Singh, J.; Kaur, L.; Sodhi, N.S.; Gill, B.S. Morphological, thermal and rheological properties of starches from different botanical sources. *Food Chem.* **2003**, *81*, 219–231. [CrossRef]
260. Vandeputte, G.E.; Vermeylen, R.; Geeroms, J.; Delcour, J.A. Rice starches. II. Structural aspects provide insight into swelling and pasting properties. *J. Cereal Sci.* **2003**, *38*, 53–59. [CrossRef]
261. Donald, A.M. Plasticization and self assembly in the starch granule. *Cereal Chem.* **2001**, *78*, 307–314. [CrossRef]
262. Perry, P.A.; Donald, A.M. The role of plasticization in starch granules assembly. *Biomacromolecules* **2000**, *1*, 424–432. [CrossRef] [PubMed]
263. Waigh, T.A.; Gidley, M.J.; Komanshek, B.U.; Donald, A.M. The phase transformations in starch during gelatinisation: A liquid crystalline approach. *Carbohydr. Res.* **2000**, *328*, 165–176. [CrossRef]
264. Vamadevan, V.; Bertoft, E.; Soldatov, D.V.; Seetharaman, K. Impact on molecular organization of amylopectin in starch granules upon annealing. *Carbohydr. Polym.* **2013**, *98*, 1045–1055. [CrossRef] [PubMed]
265. Bertoft, E.; Annor, G.A.; Shen, X.; Rumpagaporn, P.; Seetharaman, K.; Hamaker, B.R. Small differences in amylopectin fine structure may explain large functional differences of starch. *Carbohydr. Polym.* **2016**, *140*, 113–121. [CrossRef] [PubMed]
266. Shen, X.; Bertoft, E.; Zhang, G.; Hamaker, B.R. Iodine binding to explore the conformational state of internal chains of amylopectin. *Carbohydr. Polym.* **2013**, *98*, 778–783. [CrossRef] [PubMed]

267. Manion, B.; Ye, M.; Holbein, B.E.; Seetharaman, K. Quantification of total iodine in intact granular starches of different botanical origin exposed to iodine vapor at various water activities. *Carbohydr. Res.* **2011**, *346*, 2482–2490. [CrossRef] [PubMed]
268. Saibene, D.; Seetharaman, K. Use of iodine as a tool to understand wheat starch pasting properties. *Starch/Stärke* **2008**, *60*, 1–7. [CrossRef]
269. Saibene, D.; Seetharaman, K. Segmental mobility of polymers in starch granules at low moisture contents. *Carbohydr. Polym.* **2006**, *64*, 539–547. [CrossRef]
270. Tetlow, I.J. Starch biosynthesis in developing seeds. *Seed Sci. Res.* **2011**, *21*, 5–32. [CrossRef]
271. Borovsky, D.; Smith, E.E.; Whelan, W.J.; French, D.; Kikumoto, S. The mechanism of Q-enzyme action and its influence on the structure of amylopectin. *Arch. Biochem. Biophys.* **1979**, *198*, 627–631. [CrossRef]
272. Haworth, W.N.; Hirst, E.L.; Isherwood, F.A. Polysaccharides. Part XXIII. Determination of the chain length of glycogen. *J. Chem. Soc. Chem. Commun.* **1937**, 577–581. [CrossRef]